Running the gauntlet: connectivity between natal and nursery areas for Pacific ocean perch (*Sebastes alutus*) in the Gulf of Alaska, as inferred from a biophysical individual-based model

William T. Stockhausen[a*], Kenneth O. Coyle[b], Albert J. Hermann[c,d], Miriam Doyle[c], Georgina A. Gibson[e], Sarah Hinckley[a,c], Carol Ladd[d], Carolina Parada[f,g]

[a]*National Marine Fisheries Service, NOAA, 7600 Sand Point Way NE , Seattle, WA 98115-6349*
[b]*Institute of Marine Science, University of Alaska, Fairbanks, AK 99775-7220*
[c]*Joint Institute for the Study of the Atmosphere and Ocean, University of Washington, Seattle WA 98195*
[d]*NOAA/PMEL, 7600 Sand Point Way NE, Seattle, WA 98115-6349*
[e]*International Arctic Research Center, University of Alaska Fairbanks, PO Box 757340, Fairbanks, AK 99775*
[f]*Departamento de Geofísica, Universidad de Concepción, Casilla 160-C, Concepción, Chile*
[g]*Instituto Milenio de Oceanografía, Universidad de Concepción, Concepción, Chile*

ABSTRACT

Little is known regarding the importance of early-life transport and dispersion mechanisms in determining recruitment variability for Pacific ocean perch (POP) in the Gulf of Alaska (GOA). These mechanisms influence the degree of, and variability in, connectivity between offshore natal areas (parturition sites) and inshore demersal nursery habitats for young-of-the year juveniles, and may thus play an important role in the "gauntlet" that individuals must survive from parturition to recruitment. As a first attempt to assess interannual variability in connectivity between natal and nursery areas for POP in the GOA in a synthetic manner, we developed a coupled biophysical individual-based model (IBM) for POP early life history and dispersal with simple representations of active vertical movement, passive horizontal movement, growth, and settlement in appropriate nursery habitat to integrate known early-life traits with variability in environmental forcing. We used an oceanographic model for the GOA based on the Regional Ocean Modeling system (ROMS) to provide the underlying daily physical environment to force the IBM for 1996-2011 and simulated hundreds of thousands of individual POP from parturition

along the shelf break to settlement in inshore demersal nursery habitats as young-of-the-year. We used the IBM results to assess spatial patterns of annual "maximum potential" connectivity between presumed natal and nursery areas at alongshore scales of ~150 km, as well as the interannual variability in these patterns.

Results showed that, even in the absence of mortality, most (> 70%) individuals were unsuccessful in dispersing from presumed natal areas along the continental shelf break to inshore nursery areas. For those that were successful, connectivity was directed in a counterclockwise fashion (southeast to northwest) around the GOA following prevailing current patterns. Typical dispersion distances were on the order of 100's of km alongshore, much larger than those inferred from genetic sampling. Natal areas from which the highest fractions of successful individuals originated were in the southeast GOA, while the nursery areas most frequently reached by those successful individuals were in the central GOA. POP from natal areas in the western GOA were consistently exported from the system and likely contribute little to the GOA population, although they may contribute to populations in the Aleutian Islands and eastern Bering Sea. We also found that annual indices derived from the connectivity matrices were not very strongly related to any of a suite of basin- and regional-scale environmental indices, reflecting the overall complexity and scale of the pathways POP in the GOA may undertake during their early life stages and suggesting that multiple drivers operating at different spatial and temporal scales influence connectivity patterns. Finally, while our results indicate that interannual variability in physical transport may have a substantial impact on connectivity, we found little support for the hypothesis that this alone drives variability in POP recruitment.

Keywords: USA, Alaska, Gulf of Alaska, Sebastes alutus, Pacific ocean perch, recruitment, individual-based model

*Corresponding author.
E-mail address: william.stockhausen@noaa.gov. (W. T. Stockhausen)

List of Abbreviations

Abbreviation	Description
AICc	Akaike Information Criterion, adjusted for small sample sizes
AO	Arctic Oscillation
CFRS	Climate Forecast System Reanalysis
CGOA	Coastal GOA (ROMS model grid)
CPA	copepod production anomaly
CSF	cross-shelf flow
DisMELS	Dispersal Model for Early Life Stages
ENSO	El Nino/Southern Oscillation
EOF	empirical orthogonal function
ETOPO5	Earth Topography 5' grid
GOA	Gulf of Alaska
IBM	individual-based model
IERP	Integrated Ecosystem Research Project
MEI	Multivariate ENSO Index
NEP	Northeast Pacific (ROMS model grid)
NMFS	National Marine Fisheries Service
NOAA	National Oceanic and Atmospheric Administration
NPac	North Pacific (ROMS model grid)
NPRB	North Pacific Research Board
NPZ	Nutrient/Phytoplankton/Zooplankton
PC	principal component
PDO	Pacific Decadal Oscillation
POP	Pacific ocean perch
PPA	primary production anomaly
PWI	Prince of Wales Island
PWS	Prince William Sound
ROMS	Regional Ocean Modeling System
SL	standard length
WCS	water column stability

1. Introduction

The Gulf of Alaska Integrated Ecosystem Program (GOAIERP) was a vertically-integrated study of the physics, fisheries and ecosystem of the Gulf of Alaska (GOA). The goal of the program was to identify how physical and biological variability affect the recruitment of five commercially-important groundfish species in the GOA: Pacific ocean perch (POP; *Sebastes alutus*), arrowtooth flounder (*Atheresthes stomias*), Pacific cod (*Gadus macrocephalus*), walleye pollock (*Gadus chalcogramma*), and sablefish (*Anaplopoma fimbria*). The working hypothesis adopted for the GOAIERP was that the survival of the earliest life stages of groundfishes, during transport from offshore natal areas to nearshore young-of-the-year nursery habitats, is the principal influence affecting variability in subsequent recruitment to the population. As such, successful recruitment may be dependent on many interrelated factors affecting young groundfish along transport pathways from offshore natal areas to settlement in nearshore nursery habitats, including those directly influencing survival (such as food supply, competition and predation) as well as those influencing the physical environment and thus the pathways themselves (e.g. freshwater runoff, mixing and stratification, water temperature, and wind speed and direction). We refer to these biophysical processes occurring along, and influencing, the transport pathways during the first year of life as “the gauntlet”.

From the perspective of physical transport, the GOA is a highly dynamic ecosystem. Circulation in the GOA is predominantly east to west (counterclockwise). Along the continental shelf break of the northern GOA, the Alaskan Stream is a westward flowing boundary current with flow rates up to 80-100 cm s^{-1} (Reed, 1984). On the shelf, within about 50 km of the coast, the Alaska Coastal Current is a westward-flowing buoyancy-driven current with flow rates of 25

to 175 cm s^{-1} (Stabeno et al., 1995; Royer, 1998; Stabeno et al., 2004; Stabeno et al., 2015a). In the eastern GOA, the wide and variable Alaska Current flows northward along the shelf break, while the Alaska Coastal Current flows northward along the shelf. The narrowness of the shelf in the eastern GOA results in strong interaction between the shelf-break flow and the coastal current (Stabeno et al. 2015b). Both the shelf-break currents and the coastal current can meander and shed eddies, affecting the trajectories and mixing of water masses (Janout et al., 2009; Ladd and Stabeno, 2009; Ladd et al., 2005; Okkonen, 2003). Storms generated by the Aleutian Low atmospheric pressure system promote onshore advection of surface water (Cooney, 1986) and the coastal mountain range constrains these pressure systems and results in elevated precipitation and runoff (Royer, 1982). Variation in the storms and runoff result in inter-annual variability in the circulation and onshore advection.

POP, the focal species for this paper, is broadly distributed around the rim of the North Pacific in an arc from southern California north to the Bering Sea and west to northern Japan. The species is most abundant in northern British Columbia, the GOA, and the Aleutian Islands (Allen and Smith, 1988). Adults are found primarily on the upper continental slope and outer continental shelf. Most of the population occurs in patchy, localized aggregations (Hanselman et al., 2001). Genetic evidence from British Columbia and the GOA supports the existence of distinct subpopulations at small geographic scales (Withler et al., 2001; Palof et al., 2011; Kamin et al., 2013). However, adults appear to undergo seasonal migrations to shallower depths (150-300 m) during the summer for feeding, returning to the outer shelf/upper slope for mating in late fall/early winter (Love et al., 2002). POP are generally considered to be semi-demersal as they often move off-bottom during the day following diel euphausiid migrations (Brodeur; 2001). They are mostly planktivorous (Carlson and Haight, 1976; Yang, 1993; Yang and Nelson, 2000;

106 Yang et al., 2006). Juveniles feed on an equal mix of calanoid copepods and euphausiids
107 (Carlson and Haight, 1976), while larger juveniles and adults feed primarily on euphausiids, and
108 to a lesser degree, copepods, amphipods and mysids (Yang and Nelson, 2000). POP and walleye
109 pollock possibly compete for the same euphausiid prey, because euphausiids make up about 50%
110 of the pollock diet (Yang and Nelson, 2000). Large removals of POP from the GOA by foreign
111 fishing fleets in the 1960s may have allowed walleye pollock stocks to greatly expand in
112 abundance (Hulson et al., 2015).

113 POP are members of the *Sebastes* genus, a primitive viviparous group with females
114 extruding larvae rather than eggs (Love et al. 2002). Insemination occurs in the fall, and sperm
115 are retained within the female until fertilization takes place 2-5 months later (Westrheim, 1975;
116 Conrath and Knoth, 2013). Females can carry many fertilized eggs (10^4-10^6; Kendall and Lenarz,
117 1987; Haldorson and Love, 1991). The eggs develop and hatch internally, receiving at least some
118 nourishment directly from the mother. Parturition, the release of larvae, occurs in April-May in
119 the GOA (Westrheim, 1975; Conrath and Knoth, 2013). In British Columbia, adult females
120 migrate to the mouths of submarine canyons and release their larvae at depth (500-700 m; Love
121 et al., 2002).

122 The early life history of POP is not well understood (Love et al., 2002). Newly-extruded
123 larvae are ready to begin feeding, and at 3-7 mm SL are comparable in size to first-feeding larvae
124 of species with planktonic eggs (Kendall and Lenarz, 1987). Larvae are thought to be pelagic and
125 drift with the current (Ainley et al., 1993). Evidence from upwelling regions of the west coast of
126 North America suggests that rockfish larvae occupy the near-surface layers and do not migrate
127 on a diel basis (Ahlstrom, 1959; Boehlert et al., 1985; Sakuma et al., 1999; Matarese et al.,
128 2003). However, Love et al. (2002) report that studies in British Columbia have shown that

129 larvae remain at depth for a month or more prior to moving to shallower depths. The larval stage
130 in the GOA is complete at ~20 mm SL, with a duration of 1-2 months (Matarese et al., 2003).
131 Postlarval and early young-of-the-year POP have been identified using genetic techniques in
132 offshore, surface waters of the GOA (Gharrett et al., 2002). Early juveniles in the GOA remain in
133 the water column for several months until fall, at which time they take up a demersal existence in
134 subtidal habitats with complex topography and extensive cover (Carlson and Haight, 1976;
135 Carlson and Straty, 1981). At both the larval and juvenile stage, individuals cannot be
136 distinguished among several congeners without genetic identification, so most available early life
137 history information probably represents a combination of characteristics from several species
138 (Westerheim, 1975; Matarese et al., 2003; Kendall et al., 2007). The existence of distinct
139 subpopulations at small geographic scales in the GOA, noted previously, suggests that dispersion
140 in the larval and pelagic juvenile stages must be geographically limited (Palof et al., 2011;
141 Kamin et al., 2013).

142 In addition to a comprehensive field program, the GOAIERP included a modeling
143 component that integrated a suite of oceanographic, lower trophic level, and individual-based
144 modeling tools to provide broader spatial and temporal contexts to assess the impact of
145 environmental variability on processes potentially influencing recruitment of the five focal
146 groundfish species than was possible to achieve in the field program. For POP, we developed a
147 coupled biophysical, individual-based model (IBM) incorporating known early-life
148 characteristics up to the young-of-the-year stage, as well as important forcing mechanisms
149 influencing the physical environment in the GOA, to address a simplified version of the gauntlet
150 hypothesis, namely that *'recruitment variability for POP is primarily influenced by variability in*
151 *the proportion of young fish transported from offshore natal areas to nearshore nursery areas*

(connectivity) due to interannual differences solely in the hydrography of the GOA'. Thus, as a first approximation, we ignored factors such as food supply and predation potentially affecting survival along early-life transport pathways and focused on physical processes directly affecting those pathways.

Spatially-explicit IBMs, such as the one used here, have been used in studies of recruitment (Hinckley et al., 1996; Stockhausen and Lipcius, 2003; Kim et al., 2015), marine reserves (Stockhausen et al., 2000; Stockhausen and Lipcius, 2001; Paris et al., 2004; Stockhausen and Hermann, 2007; Pelc et al., 2010), population connectivity (Cowen et al., 2006; Cowen et al., 2007; Cooper et al., 2013), and for other applications in marine ecology and fisheries. IBMs used to study recruitment typically incorporate several pelagic early life stages, with biological processes that differ among the stages. To simulate the environmental factors such as temperature, salinity and currents that affect development and transport of individuals, these IBMs can be coupled to oceanographic models. IBMs used in previous recruitment and connectivity studies have ranged from quite simple models with minimal biological processes and behavior (e.g. Stockhausen and Hermann, 2007) to relatively complex models that include detailed models of processes such as feeding, bioenergetics, growth and movement. (e.g. Hinckley et al., 1996; Hinckley et al., 2001; Megrey and Hinckley, 2001; Werner et al., 2001; North et al., 2009; Parada et al., 2010; Kim et al., 2015). The degree of model complexity often reflects the data available for a particular species, as well as the research question or focus. The IBM used here for POP incorporates multiple early life stages, stage-specific durations, simple stage-specific behaviors for vertical, and habitat-specific settlement dynamics, but it does not include more sophisticated components such as bioenergetics (feeding, growth, and survival) or directed swimming. As such, it can be considered of moderate complexity on a par with the

175 sablefish IBM developed for the GOAIERP (Gibson et al., this volume).

176 Using the IBM, we quantified potential patterns of, and interannual variability in,
177 connectivity between POP natal and nursery areas over a 16-year period (1996-2011). Because
178 the IBM did not include mortality processes along individual trajectories, we refer to this as
179 "maximum potential" connectivity. We also tested relationships between connectivity and a suite
180 of environmental factors to try to identify mechanisms driving model-predicted variability in
181 connectivity. Finally, we derived potential indices of recruitment from the IBM results and
182 compared these to estimates of recruitment from the 2015 stock assessment (Hulson et al., 2015)
183 for POP in the GOA to assess the hypothesis that variability in recruitment is primarily driven by
184 variability in transport-driven connectivity.

185

2. Methods

2.1. The IBM

2.1.1. General description

To explore connectivity between offshore natal (parturition) and inshore nursery areas for POP in the GOA, we developed a species-specific IBM for POP coupled to a hydrodynamic model of the region. The POP IBM used daily-averaged output from a Regional Ocean Modeling System (ROMS; Haidevogel et al., 2008; Shchepetkin and McWilliams, 2005) model for the coastal GOA to provide the time-varying, 3-dimensional environment for the IBM. The IBM integrates biological processes affecting simulated individuals, including advective and diffusive movement using a Lagrangian particle tracking algorithm, as they develop in time through multiple early life stages. The IBM was developed using the Dispersal Model for Early Life Stages (DisMELS) framework, a platform for creating and running IBMs based on marine fish and invertebrate species with early pelagic life stages. Several other IBMs have been developed using DisMELS, including ones for northern rock sole (Cooper et al., 2013), market squid (Kim et al., 2015), arrowtooth flounder (Stockhausen et al., this volume), Pacific cod (Hinckley et al., this volume), and sablefish (Gibson et al., this volume).

2.1.1.1. ROMS

ROMS is a modeling system for developing time-varying, three-dimensional (3D) regional ocean circulation models. Details of the modeling system can be found in Haidvogel et

208 al. (2008) and Shchepetkin and McWilliams (2005), as well as on the ROMS website[1]. We used
209 a set of ROMS models that were implemented on a series of nested grids of increasing spatial
210 resolution. Each model supplied the initial and boundary conditions for the model on the next
211 finest grid. The models used were the (outermost) North Pacific (NPac) ROMS model at 20-40
212 km resolution, the Northeast Pacific (NEP) ROMS model at 10 km resolution, and the
213 (innermost) coastal GOA (CGOA) ROMS model at 3 km resolution. Validation studies and
214 detailed descriptions of related versions of the NEP model are available in Danielson et al.
215 (2011) and Hermann et al. (2009a); validation studies and detailed descriptions of related
216 versions of the CGOA model are given in Hermann et al. (2009b), Hinckley et al. (2009),
217 Dobbins et al. (2009), and Coyle et al. (2012, 2013). Key features of the NEP and CGOA models
218 are briefly summarized below.

219 The NEP model domain stretches from Baja California to the Chuckchi Sea, from the
220 coast to approximately 2000 km offshore, with a total of ~200 x 500 grid points. The CGOA
221 domain (Fig. 1) has open ocean boundaries, which allows entry and exit of the currents across its
222 boundaries. The CGOA grid has 42 vertical (stretched-coordinate, or "sigma") levels, with levels
223 more concentrated near the surface. The grid's surface layer is ~ 0.3 m in the shallowest areas
224 (10 m deep), and 15 m over the basin (6000 m deep). Bathymetry was derived from ETOPO5
225 (NGDC, 1988) and finer-scale bathymetric data. Vertical mixing in each model was based on the
226 algorithms of Large et al. (1994). Tidal dynamics were included in the CGOA model; the explicit
227 inclusion of tidal flows allows tidally-generated mixing and tidal residual flows to develop. Tides
228 were not included in the NEP simulation.

229 The NEP model was forced by 6-hourly atmospheric (for surface forcing) and monthly

[1] https://www.myroms.org/

oceanic (for initial and boundary conditions) reanalysis output from NOAA's global Climate Forecast System Reanalysis (CFSR; Saha et al., 2010), spanning the years 1995-2012. Horizontal resolution for the CFSR atmospheric and oceanic reanalyses were ~ 40 km; these were spatially-interpolated to the regional grids. Bulk forcing, based on the algorithms of Large and Yeager (2008), were used to relate the 6-hourly CFSR atmospheric variables (wind velocities, air temperature, rainfall rate, absolute humidity, downward shortwave and longwave radiation) to surface stress and the net transfers of sensible heat, latent heat, shortwave and longwave radiation through the sea surface, as well as surface freshening by the rainfall. The CGOA model was driven by the same atmospheric forcing as the NEP model.

All of the oceanic boundary conditions were enforced using the hybrid nudging/radiation scheme of Marchesiello et al. (2001). Whereas the NEP initial and boundary conditions were derived from CFSR, the CGOA model oceanic initial and boundary conditions were derived from weekly averages of the NEP biophysical output, spatially interpolated onto the CGOA boundaries (one-way nesting with no feedback to the outer model). The NEP model was spun up for one year prior to its use for initialization of the CGOA model. Freshwater runoff was applied to the CGOA simulation by freshening of the surface salinity field within a few gridpoints of the coastline. The climatology of Dai et al. (2009) was used to set the mean alongshore spatial pattern of the runoff; the offshore pattern was set using an exponential taper based on squared distance from the coastline, with an e-folding distance of ~30 km. This fixed spatial pattern was modulated by Royer (pers. comm.) total monthly runoff estimates for the CGOA, which are based on measured rainfall and temperature. The result was normalized to ensure that the total volumes estimated by Royer were fully distributed into the CGOA during each month. Output from the CGOA model, including 3-dimensional (3D) current, temperature and salinity fields,

253 was temporally filtered to remove tidal and inertial aliasing, and stored once per model day for
254 subsequent use in the individual-based models.
255 *2.1.1.2. DisMELS*
256 DisMELS was developed at the Alaska Fisheries Science Center (NOAA/NMFS) to
257 provide a framework to develop, and a platform to run, IBMs simulating the early life stage
258 development and dispersion of marine fishes and invertebrates with pelagic egg and larval
259 stages. DisMELS couples this individual-based biological modeling framework with stored
260 output from a ROMS oceanographic model to provide a time-varying, 3D physical environment
261 in which to simulate the dispersal trajectories of thousands of simulated eggs and larvae from
262 spawning locations through early juvenile life stages. DisMELS also provides a graphical user
263 interface to facilitate defining life stage sequences, stage-specific characteristics, and initial
264 conditions, as well as to run models and review results. DisMELS has previously been used to
265 study dispersal mechanisms in northern rock sole (Cooper et al., 2013) and market squid (Kim et
266 al., 2015).
267 We used stored daily output from the CGOA ROMS oceanographic model in its native
268 curvilinear grid formats to provide the time-varying, 3D physical environment "experienced" by
269 simulated individuals when the IBM was run. Biological processes in the IBM were integrated
270 using a 20-minute model time step to update characteristics such as size, age and life stage for
271 each "surviving" simulated individual. ROMS model fields were spatially interpolated at each
272 integration time step to the location of each simulated individual to provide *in situ* values to drive
273 advective movement and other environmentally-mediated biological processes. A 4^{th}-order
274 predictor-corrector algorithm was used to perform Lagrangian integration to update individual
275 locations on the ROMS grid. This algorithm was based on the ROMS algorithm for passive

276 drifters, but it can also incorporate individual motion due to active swimming or buoyancy
277 effects, as well as diffusive motion in the form of horizontal and/or vertical random walks.
278 Individuals that were advected beyond the boundaries of the CGOA grid did not "survive".

279 In the models run for this study, values for *in situ* temperature and salinity were also
280 interpolated at each biological time step for each individual. Information on each individual (life
281 stage, age, age-in-stage, location [latitude, longitude, depth], size, *in situ* temperature, and *in situ*
282 salinity) was saved at a daily time step for further analysis.
283
284 *2.1.2. POP IBM details*
285 At both the larval and juvenile stage, POP cannot be distinguished among several
286 congeners without genetic identification, so most available early life history information
287 probably represents a combination of characteristics from several species (Westrheim, 1975;
288 Matarese et al., 2003; Kendall et al. 2007). Thus, the POP IBM was a relatively simple IBM,
289 reflecting the limited knowledge we have for this species in its early life stages. Model processes
290 included in the IBM were similar to those in the sablefish IBM (Gibson et al., this volume):
291 growth rates in all life stages were stage-dependent constants and movement was essentially
292 passive and undirected, except that individuals moved vertically to remain within stage-specific
293 "preferred" depth ranges based on observed or presumed depth distributions.
294 The POP IBM consisted of five sequential early life stages, reflecting the conceptual
295 model depicted in Fig. 2: preflexion larva, postflexion larva, pelagic juvenile, settlement-stage
296 juvenile, and benthic juvenile. The first four stages were defined in the IBM to facilitate
297 ontogenetic changes in "preferred" depth ranges, growth rates, and movement parameters (Table
298 1). The final stage, the benthic juvenile stage, had no associated dynamics; it was simply a

299 "marker" stage that indicated an individual had successfully settled in a benthic nursery area.

300 Based on depth and size ranges for newly-extruded larvae (3-7 mm: Kendall and Lenarz,
301 1987; 3.5-7.5 mm: Matarese et al., 2003), individuals were "released" in the simulation near the
302 bottom between (nominally) the 300-600m isobaths along the shelf break as preflexion larvae at
303 4.5 mm SL (Table 1). Stage-specific depth ranges were drawn from a variety of sources, but
304 reflect observations that larvae remain at depth for the first month or so (Love et al., 2002) and
305 are then found in the upper portion of the water column above the pycnocline (Ahlstrom, 1959;
306 Lenarz et al., 1991; Larson et al., 1994; Sakuma et al., 1999; Doyle and Mier, 2016).
307 Consequently, we set the preferred depth range for the preflexion larval stage to 300-700 m,
308 consistent with the assumption that preflexion larvae remain at depth. For postflexion larvae and
309 pelagic juveniles, we set the preferred depth range to 5-40 m, such that individuals moved up in
310 the water column upon transition to the postflexion larval stage at 9 mm SL and stayed in the
311 upper water column (Table 1). Settlement-stage juveniles were given a slightly deeper preferred
312 depth range (5-50 m) consistent with their "preferred" settlement habitat (see below).

313 The postflexion larval stage ended when an individual reached 20 mm SL and
314 transitioned to the pelagic juvenile stage (Matarese et al., 1989). At 60 mm SL, pelagic juveniles
315 became settlement-stage juveniles, with the ability to adopt a more benthic lifestyle in suitable
316 nursery habitat (Moser et al., 1977). Based on assumed completion of the transition to a more
317 demersal lifestyle in the fall of the year, we allowed a 30-day window for settlement-stage
318 juveniles to become benthic stage juveniles. Lacking other habitat-related information (e.g.
319 bottom type) in the simulation, we defined preferred nursery habitat for POP as any bottom
320 shallower than the 50-m isobath. Settlement-stage juveniles that reached preferred nursery
321 habitat settled to the benthos, became benthic juveniles, and were counted as "successful".

Settlement-stage juveniles that reached the end of the 30-day window but were in an area of alternative nursery habitat, defined as any bottom between the 50 and 150 m isobaths, were also assumed to make the transition to benthic juvenile and were counted as "successful". Individuals that could not become benthic juveniles by the end of a model run (i.e. they did not reach a preferred or alternative nursery habitat by the end of the 30-day settlement window as settlement-stage juveniles, or they exited the model grid) were regarded as "unsuccessful".

Except for the transition from settlement-stage juvenile to benthic juvenile, all transitions between sequential life stages were explicitly based on individual size, such that when an individual reached the maximum size for a life stage (Table 1), it "metamorphosed" to the subsequent stage. However, stage-specific linear growth rates G_s (in mm d^{-1}; Table 1) were generally derived from published values for L_{min}^{s} and L_{max}^{s}, the stage-specific minimum and maximum sizes, and T_s, the assumed stage duration using:

$$G_s = \frac{L_{max}^{s} - L_{min}^{s}}{T_s} \quad (1)$$

The pelagic juvenile stage is assumed to last several months, and settlement to benthic nursery areas occurs in the fall (Matarese et al., 2003). For the IBM, then, we assumed that the pelagic juvenile stage lasted 90 days. Given the minimum and maximum sizes for this stage (Table 1), G_s for this stage was estimated at 0.44 mm d^{-1}, which appears to be reasonable based on growth rates for pelagic juveniles in other *Sebastes* species (Woodbury and Ralston, 1991). To obtain G_s for the pre- and postflexion larval stages, we assumed the total larval duration was 60 days (Matarese et al., 1989). We then estimated a mean intrinsic growth rate (g, in d^{-1}) across both stages using

$$g = \frac{1}{T} ln \left(\frac{L_{max}^{post}}{L_{min}^{pre}} \right) \quad (2)$$

where T was the total larval duration, and L_{min}^{pre} and L_{max}^{post} were the minimum preflexion and maximum postflexion larval sizes, respectively. Individual stage-specific durations, T_s, were then estimated from g and the stage-specific minimum and maximum sizes using:

$$T_s = \frac{1}{g} ln\left(\frac{L_{max}^{S}}{L_{min}^{S}}\right) \quad (3)$$

Finally, G_s was estimated for each stage using Equation 1, resulting in estimated pre- and postflexion larval growth rates of 0.16 and 0.34 mm day^{-1} (Table 1). Similar increases in growth rate between the pre- and postflexion stages have been observed for other *Sebastes* species (Laidig et al., 1991; Sakuma and Laidig, 1995; Woodbury and Ralston, 1991).

For lack of information, and as a simple convenience, growth of settlement-stage juveniles was ignored. As noted above, transition from the settlement stage to the benthic juvenile stage if an individual reached an area with preferred nursery habitat within a 30-day window.

Stage-specific vertical swimming speeds (Table 1) were chosen primarily to allow individuals to remain within their preferred depth ranges; they are, however, consistent with observed swimming speeds (Fisher et al., 2007; Kashef et al., 2014). Parameters governing vertical and horizontal random walks (vertical and horizontal diffusivities) were given non-zero, but relatively small values, to inject some stochasticity into the simulations.

2.1.3. Initial conditions

Because the main groundfish surveys in the GOA occur in the summer on a biennial or triennial basis, there is little information on the spatial (and interannual) patterns of the release of POP larvae during parturition across the GOA to inform initial conditions in the IBM. For each

366 model year, simulated individuals were released as preflexion larvae in a series of separate
367 "cohorts" at 5 m above the bottom within hypothetical "parturition" areas (Fig. 1) along the
368 continental shelf break. Grid cells along the continental shelf edge were classified as parturition
369 areas if the bathymetric depth at the center of the cell was between 300 and 600 m. For each
370 cohort, individuals were released at the same time on a 1-km *x* 1-km grid across the parturition
371 areas, resulting in a total 16,453 individuals per cohort.

372 The relative pattern of parturition by POP in the GOA must be inferred from observed
373 patterns of larval *Sebastes* (spp.) abundance in plankton sampling (Fig. 3a) while making some
374 assumptions as to the fraction that are actually POP. Because parturition for this species in the
375 GOA is known to occur early in the spring, while for other rockfish species it occurs later in the
376 summer, we decomposed the seasonal pattern of larval abundance in the GOA (Doyle and Mier,
377 2016) into two relatively broad distributions: one for POP and one for the other rockfish species.
378 This resulted in the relative pattern shown in Fig. 3b, which we assumed reflected relative
379 seasonal rates of parturition for POP. To incorporate this temporal pattern of parturition when we
380 calculated annual connectivity for each year, we released six cohorts of simulated preflexion
381 larvae on a bi-weekly basis and weighted individuals according to the pattern of relative
382 abundance in Figure 3b. In all, we tracked a total of 98,718 simulated individuals per model year.
383
384 *2.2. Connectivity*
385
386 Because we didn't include mortality processes along individual trajectories in the IBM,
387 as used here "connectivity" represents the *maximum* probability of being successfully transported
388 from an offshore natal area to an inshore nursery area, where individuals can "settle" to the

389 benthos and become benthic juveniles. Nursery areas that accounted for a substantial fraction of
390 successful "settlers" originating from a given natal area were considered to be "highly-
391 connected" to that natal area, while nursery areas that accounted for a small fraction of
392 successful recruits were only "weakly-connected".
393
394 *2.2.1. Connectivity zones*
395 To quantify annual connectivity between natal and nursery areas on rather broad spatial
396 scales, we divided the GOA into a coarse grid with twelve along-shelf zones (1-12) roughly 150
397 km wide and five cross-shelf depth zones (Fig. 1). The choice of spatial scale was somewhat
398 arbitrary and reflected a subjective balance between spatial resolution and uncertainty (sampling
399 error, natal and nursery habitat characterization, and mesoscale variability in the physical
400 model). We also defined a 13th "along-shelf" zone, Cook Inlet, which does not contain any natal
401 areas and is not (strictly speaking) "along-shelf". However, it does contain preferred and
402 alternative nursery areas and thus we quantified settlement within it and connectivity to it. The
403 five cross-shelf zones based on increasing bathymetric depth and assumed nursery suitability
404 were: 1) the preferred nursery zone (0-50 m), 2) the alternative nursery zone (50-150 m), 3) the
405 intermediate shelf zone (150-300 m), 4) the natal zone (300-600 m), and 5) the off-shelf zone
406 (>600 m but less than ~150 km from the shelf break; Fig. 1). We also defined a "deep-sea" zone,
407 with no division into alongshore zones, constituting the area of the GOA farther offshore than the
408 off-shelf depth zone. Using these zones, we classified each cell in the CGOA ROMS grid by the
409 alongshore zone/depth zone combination within which it fell.
410 *2.2.2. Annual connectivity matrices*
411 To estimate annual patterns of connectivity, we doubly-classified each individual in a

simulation based on 1) the alongshore zone, *s*, in which it was released (all individuals were released in the natal depth zone) and 2) the alongshore zone/depth zone in which it ended. To simplify analysis and focus on patterns of alongshore connectivity between natal and nursery areas, we aggregated individuals that successfully reached either of the depth zones within an alongshore zone (denoted here as *n*) which were assumed to function as nursery areas. Based on these doubly-classified individuals, we then estimated annual connectivity matrices $C_{n,s}(y)$ as the probability that an individual released from natal zone *s* in year *y* successfully reached a nursery area and became a benthic juvenile in alongshore nursery zone *n* using

$$C_{n,s}(y) = \frac{N_{n,s}(y)}{N_s(y)} \quad (4)$$

where $N_s(y)$ was the number of individuals released in year *y* as preflexion larvae in natal zone *s* and $N_{n,s}(y)$ was the number of those individuals that successfully recruited to nursery zone *n*. When considered as a series of annual matrices, the $C_{n,s}(y)$ thus reflect the annual spatiotemporal variability in connectivity between natal and nursery zones exhibited at alongshore scales of ~150 km.

As noted above, because we did not include mortality-related processes (e.g. starvation, predation) in the IBM, the $C_{n,s}(y)$ represent "maximum potential" connectivity because they are based solely on successful transport to benthic nursery areas. Consideration of mortality along the trajectories of "successful" individuals would further reduce the absolute scales of these matrices, but would not (to first order, at least) change the relative patterns unless mortality rates were spatially heterogeneous.

2.2.3. Aggregate connectivity indices

In order to summarize changes in the annual connectivity matrices in a simpler fashion, we calculated an aggregate annual index, $C_s(y)$, for each natal zone *s* that reflected the annual

probability of successfully reaching *any* nursery zone from that natal zone, i.e. the ratio of the number of successful individuals from natal zone *s* divided by the total number released in that zone:

$$C_s(y) = \frac{\sum_n N_{n,s}(y)}{N_s(y)} = \sum_n C_{n,s}(y) \quad (5)$$

where the second term follows from Equation 4. If recruitment variability for POP in the GOA is driven primarily by changes in transport alone, rather than changes in spawning biomass or survival of larvae along across the "gauntlet", then recruitment would be expected to be well-correlated with the $C_s(y)$, at least for those alongshore zones where the most parturition occurs.

2.3. Model validation and estimated recruitment

Few data exist with which to validate the IBM. The only suitable dataset available to compare with predictions from the IBM is the recruitment time series estimated as part of the biennial stock assessment conducted by NOAA Fisheries (Hulson et al., 2015). The stock assessment uses a statistical age-structured model for POP in the GOA to fit fishery catch and discard information, as well as several fishery-independent datasets, to estimate the annual recruitment of age-2 POP to the stock starting in 1961 (Fig. 9-14 in Hulson et al., 2015), as well as the annual abundance of older age classes and spawning stock biomass. The 2015 stock assessment estimates of age-2 recruitment (R), lagged to the age-0 year class, are shown for 1996-2011 in Fig. 4a along with the estimated spawning biomass (S). Making standard transformations to the estimated recruitment time series, such as transforming to log-scale ($\ln(R)$) or assuming a stock-recruit relationship exists ($\ln(R/S)$), had little effect on the apparent scale of variability in recruitment after standardizing the time series (Fig. 4b), so we only used

457 the standardized recruitment time series (*R*, Figure 4b) in comparisons with results from the
458 IBM.
459
460 *2.4. Analysis*
461
462 We focused analysis of the multi-year IBM results on: 1) elucidating predicted patterns of
463 connectivity, and their variability, between natal and nursery zones and 2) testing whether
464 variability in recruitment to the GOA POP stock appeared to be reflected in the connectivity
465 indices derived from the IBM.
466
467 *2.4.1. Connectivity matrices*
468 *2.4.1.1. Long-term patterns*
469 We characterized long-term connectivity between natal and nursery zones using the
470 temporal median, $\tilde{C}_{n,s}$, of the annual connectivity matrices:

$$\tilde{C}_{n,s} = \text{median}_{y\in[1996-2011]}[C_{n,s}(y)] \quad (6)$$

471 We used the median as more representative of "typical" conditions than the mean, which can be
472 influenced by extreme events. Temporal variability was estimated by calculating the temporal
473 root median square deviation, analogous to the standard deviation for a mean, from the annual
474 connectivity matrices:

$$\tilde{\sigma}_{n,s} = \sqrt{\frac{1}{16}\sum_{y=1996}^{2011}\left(C_{n,s}(y) - \tilde{C}_{n,s}\right)^2} \quad (7)$$

475

476 *2.4.1.2. EOF analysis*

477 To better elucidate spatial and temporal patterns of variability in connectivity, we
478 decomposed the time series of annual connectivity matrices $C_{n,s}(y)$ into a set of orthogonal
479 spatial modes and associated principal component (PC) time series using empirical orthogonal
480 function (EOF) analysis (Preisendorfer, 1988; von Storch and Zwiers, 1999). The modes (EOFs)
481 capture independent patterns of spatial co-variation that account for (when ranked accordingly)
482 decreasing levels of total variance, whereas the time series for each PC reflects the contribution
483 of the associated spatial mode to the total variance in year *y*. EOFs were calculated using the
484 "prcomp" function from the R statistical program (R Core Team, 2015).

485

486 *2.4.2. Environmental indices potentially associated with connectivity*

487 We next attempted to determine whether the temporal variability in predicted
488 connectivity was closely associated with any members of a set of well-known or more-easily
489 computed environmental indices. If so, then the associated indices could suggest important
490 mechanisms influencing variability in predicted connectivity and/or provide proxies for the
491 indices derived from the IBM. Because our measure of connectivity here was "maximum
492 potential" connectivity (i.e. it did not incorporate mortality processes or variability in growth),
493 we confined our analysis to two suites of physical environmental indices that reflect variability in
494 transport processes: 1) several standard, large-scale climate indices important for the North
495 Pacific and 2) a set of smaller-scale indices of cross-shelf transport derived from the ROMS
496 models used to drive the IBM.

497 The first set of environmental indices we considered consisted of climate indices known

498 to reflect important large-scale environmental processes in the north Pacific Ocean and GOA
499 (see Fig. S1 in the Supplementary Material). These, or similar, indices have been weakly linked
500 to variability in recruitment to the POP population (Stachura et al., 2014). Thus, it was of interest
501 to test whether we could detect any relationship between these indices and IBM-predicted
502 indices of connectivity. We considered seasonally-averaged (spring, summer, fall) time series of
503 the Arctic Oscillation[2] (AO; Higgins et al., 2000, 2001, 2002), the Pacific Decadal Oscillation[3]
504 (PDO; Mantua et al., 1997; Zhang et al., 1997; Bond and Harrison, 2000), and the Multivariate
505 El Nino-Southern Oscillation Index[4] (MEI; Wolter and Timlin, 1993, 2011). The AO reflects a
506 climate pattern characterized by winds circulating counterclockwise around the Arctic at ~55°N
507 latitude. A positive AO indicates strong winds circulating around the North Pole which confine
508 colder air to the polar regions. A negative AO, on the other hand, means that this belt of winds is
509 weaker, which allows for southward movement of colder, arctic air and increasing storminess in
510 mid-latitudes. The PDO reflects the leading principal component of monthly sea surface
511 temperature (SST) anomalies in the North Pacific; a positive PDO means warmer-than-usual
512 conditions, whereas a negative PDO means colder SSTs. The MEI characterizes the El Niño/La
513 Niña state of the Pacific Ocean: a negative MEI indicates La Niña conditions and weaker gyre
514 circulation in the GOA, whereas a positive MEI indicates El Niño conditions and stronger gyre
515 circulation in the GOA (Hermann et al., 2016).

516 The second set of indices we considered were 9 regional-scale, seasonal indices of cross-
517 shelf flow (CSF) derived directly from the ROMS models used to drive the IBM (see Fig. S2 in
518 the Supplementary Material). These were calculated for 1997-2011 using the coarser-scale NEP

[2] http://www.cpc.ncep.noaa.gov/products/precip/CWlink/daily_ao_index/monthly.ao.index.b50.current.ascii.table
[3] http://jisao.washington.edu/pdo/PDO.latest
[4] http://www.esrl.noaa.gov/psd/enso/mei/table.html

519 ROMS model output that provided the boundary conditions for the higher resolution CGOA
520 ROMS model runs. Using the bathymetry for the NEP model, the latitude of the 500-m isobath
521 was found at each longitude in the model grid and smoothed using a 5-point (0.3°) boxcar filter
522 to eliminate small-scale corners. Monthly-averaged velocities from the NEP model run were then
523 interpolated to locations along the smoothed 500 m isobath. The resulting eastward and
524 northward components of velocity were rotated into the local on-shelf and cross-shelf direction
525 at each location. Monthly climatologies were calculated for 1997-2011 and removed to obtain
526 monthly anomalies from the climatological seasonal cycle. These anomalies were then averaged
527 across each of three regions (West: 155°-150°W, Central: 150°-145°W, and East: 145°140°W)
528 and three seasonal time periods (spring: Apr-Jun; summer: Jul-Sep; fall: Oct-Dec).

529 All indices were converted to z-scores prior to analysis. We did not include winter (Jan-
530 Mar) for any of the environmental indices in our analysis because larval and pelagic-stage
531 juvenile POP are not in the water column during this period.

532 We limited our analysis to the aggregate connectivity indices reflecting settlement
533 success by natal zone (i.e. the $C_s(y)$), as well as the time series of scores from the first two
534 principal components in the EOF analysis. We tested the environmental indices as potential
535 predictors of the aggregate connectivity indices using simple linear models of the form $\tilde{I}_s(y) =$
536 $\beta_i \cdot \tilde{F}_i(y) + \beta_j \cdot \tilde{F}_j(y)$, where $\tilde{I}_s(y)$ denotes the standardized (as z-scores) time series for the
537 aggregated connectivity index $C_s(y)$ from the IBM and $\tilde{F}_i(y)$ denotes the standardized time
538 series for the *i*th potential predictor. The β_is are equivalent to the correlation coefficient between
539 the two time series in the case of a one-factor model (i.e. where $\beta_j \equiv 0$).

540 For each connectivity index, we evaluated all possible single-factor and two-factor

541 models using the "glmulti" package (Calcagno and de Mazancourt, 2010) and the "lm" function
542 in R (R Core Team, 2015). W determined the "best" model using AICc, the Akaike Information
543 Criterion adjusted for small sample sizes (Burnham and Anderson, 2002). To determine the
544 significance of this model, it was necessary to correct the reported p-value for the "best" model
545 in light of the large number (~300) of multiple comparisons made during the model selection
546 process. Because of the lack of independence among the multiple comparisons involved in this
547 analysis, we could not use the standard Bonferroni correction to the p-value. Instead, we
548 empirically estimated the family-wise p-value associated with the "best" model by ranking the
549 model's F-statistic among those obtained by repeating the analysis 10,000 times using randomly-
550 generated, normally-distributed time series as substitutes for the response and all covariates. The
551 empirical p-value was taken as *1-n/N*, where *n* was the rank of the model's F-statistic and *N* was
552 10,000.
553
554 *2.4.3. Connectivity indices as predictors of recruitment*
555 Finally, we tested the aggregate connectivity indices $C_s(y)$ as potential predictors for
556 recruitment using simple linear models of the form $\tilde{R}(y) = \sum_i \beta_i \cdot \tilde{I}_i(y)$, where $\tilde{R}(y)$ denotes
557 the standardized (as z-scores) annual recruitment time series from the stock assessment model
558 (Hulson et al., 2015), β_i is the *i*th regression parameter, and $\tilde{I}_i(y)$ denotes the *i*th standardized
559 connectivity index time series. This form would be consistent with the hypothesis that
560 recruitment variability really was driven by variability in connectivity if the spatial pattern of
561 parturition (larval release) across the GOA did not change substantially during 1996-2016. In this
562 case, the β_is would reflect the spatial pattern of parturition.
563 As an exploratory analysis, we evaluated all possible 1-zone, 2-zone, and 3-zone

564 combination models using the “glmulti” package (Calcagno and de Mazancourt, 2010) and the
565 “lm” function in R (R Core Team, 2015). As with the previous analysis, we selected the “best”
566 model using AICc (Burnham and Anderson, 2002). We also used the approach outlined in the
567 previous section to determine an empirical p-value for the “best” model.

568 **3. Results**

569

570 *3.1. IBM output*

571

572 As noted previously, individuals were released on a 1-km *x* 1-km grid across parturition
573 areas defined as ROMS grid cells with bathymetric depths between 300 and 600 m, with a total
574 of 16,453 individuals released per cohort, and six cohorts per year. Because actual release depths
575 on the 1-km *x* 1-km grid were interpolated within each ROMS grid cell classified, individual
576 release depths spanned a somewhat wider range than 300-600 m—about 11% of simulated
577 preflexion larvae were released outside this nominal interval (Figure S3 in the Supplementary
578 Material).

579 Most simulated individuals exhibited a general trend to move to the north and west
580 during the model runs, but individual trajectories were complex, indicating the influence of
581 mesoscale and larger eddies on their movement (Fig. 5). Almost all individuals remained off the
582 shelf in deeper water as preflexion larvae, and were not transported onto the shelf until they
583 reached the postflexion larval stage and moved up in the water column (nominally 5-40 m
584 depths). Many individuals that were not successful in recruiting to suitable nursery habitat during
585 the allotted time frame were transported further off shelf (away from nursery habitats) into the
586 deep ocean zone *vis-a-vis* most "successful" individuals; successful individuals tended to move
587 onto and stay on the shelf, although a large fraction (40-50%) of these were also transported off
588 the shelf only to return on-shelf via eddies and gyres. While some individuals that were released
589 in the southeast (natal zones 1-4) exited the model grid at its southeast boundary, many more
590 exited the grid at its western boundary due to the general counter-clockwise nature of the mean

591 circulation along the shelf. Individuals that exited the grid were classified as unsuccessful.

592 Only a relatively small fraction of simulated individuals successfully recruited to nursery
593 areas, particularly if they were released west of PWS (zone 6; Fig. 6a). As a result of the general
594 circulation pattern, and because of its proximity to the western boundary of the model grid,
595 individuals released in natal zone 12 (West Shumagins) were successful in only one modeled
596 year (1998; Fig. 6a). Simulated individuals released in the eastern half of the GOA (natal zones
597 1-6) were much more likely to reach nursery areas in the allotted time than those released in the
598 western half (zones 7-12), while interannual variability in the fraction successful from any natal
599 zone, $C_s(y)$, was large relative to the mean.
600
601 *3.2. Connectivity matrices*
602
603 *3.2.1. Long-term patterns*
604 The cell-by-cell median and root median square deviation of the annual connectivity
605 matrices (Fig. 7) indicate that the highest median connectivity (22%) was between natal zone 3
606 (Cross Sound) and nursery areas in zone 6 (PWS). Natal zones 1, 2, 4 and 5 (PWI, Sitka, Yakutat
607 and Icy Bay) were also relatively highly connected to nursery areas in zone 6 (>10% each).
608 Median connectivity was directed in a counterclockwise fashion, with parturition areas in the
609 south and east (lower number alongshore zones) connected with nursery areas to the north and
610 west (higher number alongshore zones). This was also reflected in the average nursery zone
611 reached by successful individuals from natal zone *s*, $\overline{N}_s(y)$ (Fig. 6b). While some retention
612 occurred for natal zones in the east (areas 1-6), the level was generally quite small (< 2%, except
613 for natal zone 2, which exhibited 3% median retention). For natal zones in the west (areas 7-12),

614 median retention was essentially zero. Median connectivity from west to east (clockwise
615 transport) was negligible, even for adjacent areas, although the pathways in Fig. 5 indicate
616 clockwise transport does occur, sometimes on the order of 400-600 km along the shelf. Temporal
617 variability was generally positively correlated with median connectivity, so the most highly-
618 connected cells also exhibited the highest variability (Fig. 7b).
619 The single highest fraction of individuals recruiting from a natal zone (s) to nursery areas
620 in an alongshore zone (n) was 32% in 2002 for 3→6 (see Fig. S4 in the Supplementary
621 Material), that is, from s = 3 (Cross Sound) to n = 6 (PWS). In fact, this pathway accounted for
622 the highest 8 connectivity values over all 16 simulated years. The other pathways that accounted
623 for the top ten values over all years were 2→6 (one year) and 4→6 (one year). Thus, the most
624 highly connected natal zones were separated by approximately 850 km (2: Sitka), 650 km (3:
625 Cross Sound), and 425 km (4: Yakutat) from the most highly-connected nursery zone (6: PWS).
626
627 *3.2.2. EOF analysis*
628 The first two EOFs of the annual connectivity matrices accounted for 60% of the total
629 variance, with much smaller contributions from additional components. Positive scores on the
630 first EOF were associated with somewhat higher connectivity between a natal zone and its
631 neighbors immediately to the north or west, but lower connectivity between the same natal zone
632 and more distant zones moving counterclockwise around the GOA (Fig. 8), possibly reflecting
633 an slowdown in the overall counterclockwise flow in the GOA. Positive scores on the second
634 EOF primarily reflected higher connectivity between natal zones east of zone 6 (PWS) with
635 nursery areas in PWS.

636 *3.3. Aggregate connectivity indices*

637

638 *3.3.1. Time series*

639 As noted in Section 3.1, the annual total fraction of individuals originating from natal
640 zone *s* that successfully reached nursery areas anywhere in the GOA, $C_s(y)$, was substantially
641 higher, and exhibited more variability, for natal zones in the eastern GOA compared with those
642 in the west (Figs. 6a and 9). The largest fraction of successful individuals came from natal zone 3
643 (Cross Sound) in 1999, when almost 71% of individuals originating in this zone successfully
644 reached nursery areas somewhere in the GOA. In contrast, fewer than 0.2% of individuals
645 originating in natal zones 11 and 12 (East and West Shumagins, respectively) successfully
646 reached nursery areas in 15 out of the 16 model years. Because few successful individuals
647 originated from these two natal zones, these were dropped from subsequent analysis.

648

649 *3.3.2. Linear model analysis for environmental indices potentially associated with connectivity*

650 We found little evidence for any strong relationships between the aggregate connectivity
651 indices (the annual total fraction of successful individuals from natal zone *s,* $C_s(y)$, and the 2
652 PC's) and any of the 18 seasonal large-scale (AO, MEI, PDO) or the regional-scale (ROMS-
653 derived cross-shelf flow) environmental indices we considered as potentially-explanatory drivers
654 (Table 2). The only model for the $C_s(y)$ with an adjusted R^2 of 50% or better was that for zone 1
655 (PWI), which appeared to be positively related to deviations in cross-shelf flow in the eastern
656 GOA during spring and negatively related to deviations in the springtime AO (Table 3).
657 However, this model was not statistically significant ($p = 0.06$, after adjustment for multiple
658 comparisons). The same two indices were also found to be potentially associated with changes in

659 PC 1, the temporal loadings on the first EOF, with an adjusted R^2 of 50% (Table 3). Again,
660 though, the model was not statistically significant (the p = 0.31 for this model).
661
662 *3.4. Connectivity and recruitment*
663
664 *3.4.1. Time series*
665 During the years for which the IBM was run, estimated recruitment from the 2015 stock
666 assessment was episodic, with high points in 1998 and 2006 and low points in 1996, 2003, and
667 2009 (Fig. 4a; Hulson et al., 2015). In contrast, estimated spawning biomass steadily increased
668 between 1996 and 2011, from 82,000 t to 150,000 t (Fig. 4a). However, the time series for ln-
669 scale recruits-per-spawning biomass ($\ln(R/S)$), standardized as z-scores, was quite similar to the
670 standardized time series for both R and $\ln(R)$ (Fig. 4b). As a consequence, we used the
671 standardized time series for R to perform subsequent analyses.
672
673 *3.4.2. Linear model analysis for aggregate connectivity indices as predictors for recruitment*
674 Deviations in POP recruitment as estimated by the 2015 stock assessment (Fig. 4b;
675 Hulson et al., 2015) were reasonably well-explained by a linear model based on z-scores for the
676 IBM-predicted annual total fraction of successful individuals, $C_s(y)$, from natal zones 2 and 6
677 (Sitka and PWS, respectively; Table 4, Fig. 10). The adjusted R^2 for this "best" model was 62%;
678 it was marginally significant, with an empirical p-value of 0.044. Deviations in $C_2(y)$ were
679 positively associated with deviations in recruitment (coefficient = 0.55), but deviations in $C_6(y)$
680 were negatively associated with deviations in recruitment (coefficient = -0.64).
681

682 **4. Discussion**

683

684 The guiding hypothesis of the GOAIERP program was that successful recruitment of
685 POP is primarily determined by processes which occur during the larval and early juvenile
686 stages, in the "gauntlet" between extrusion in offshore natal areas and settlement in nearshore
687 nurseries as young-of-the-year. Of the many interrelated processes that can occur during this
688 period, our study focused on whether variability in transport mechanisms, as reflected in
689 variability in connectivity between offshore natal zones and inshore nursery habitats, could
690 account for subsequent variability in recruitment. We used linked models, specifically, a regional
691 oceanographic model, and a species-specific, Lagrangian IBM to address this issue.

692 The POP IBM described here was an attempt to combine current knowledge regarding
693 early-life processes at the individual and population-level (e.g. growth, seasonality of parturition)
694 with ecosystem-level mechanisms (e.g. current patterns) in a synthetic fashion across
695 spatiotemporal scales from centimeters and minutes to 100s of kilometers and months-to-years in
696 order to assess the extent to which variability in passive physical transport from offshore natal
697 areas to nearshore juvenile nurseries could account for subsequent variability in recruitment to
698 the population. Lacking information on variability in mortality processes along individual
699 trajectories, we focused our analysis of results from the IBM on estimating "maximum potential"
700 connectivity between offshore natal areas and nearshore nursery habitats at alongshore spatial
701 scales on the order of 150 km. Although "maximum potential" connectivity does not include
702 mortality processes acting along individual pathways, it does incorporate variability in transport
703 processes and seasonality in parturition. Estimates of even such a narrowly-defined version of
704 connectivity can generate hypotheses regarding the fate of individual fish extruded in particular

705 regions, the potential importance of different natal and nursery areas, and the impacts of larger
706 scale climate forcing on these patterns. Lagrangian IBMs are one of the few available tools for
707 predicting connectivity, with their ability to follow individuals along transport pathways.
708
709 *4.1. Individual pathways*
710
711 Results from the IBM suggest that, as young POP progress through early pelagic life
712 stages from newly-extruded larva to newly-settled, young-of-the-year benthic juvenile, there is a
713 predominant pattern of counter-clockwise (southeast to northwest) transport along the
714 continental shelf, as successfully-settling individuals move from deeper parturition areas along
715 the shelf break to shallower, inshore nursery areas (e.g. Figs. 5 and 6b). Individual pathways are
716 complex, indicating the influence of mesoscale and larger eddies on their movement. Many
717 individuals are transported off the shelf, although some of these are also transported back onto
718 the shelf. The tortuous nature of the pathways illustrated in Fig 5 has strong implications for
719 larval surveys conducted in the GOA, particularly regarding the inherent uncertainty regarding
720 the origin or destination of individuals collected during such cruises. Most individuals (typically
721 >70%) in the model runs were not successful in reaching inshore nursery habitat from offshore
722 natal zones. Many of these "unsuccessful" individuals were transported beyond the modeled
723 area, particularly to the northwest, suggesting the GOA population may provide recruits to
724 populations in the Aleutian Islands or the eastern Bering Sea.
725
726 *4.2. Connectivity*
727

728 The highest fraction of individuals that successfully settled in inshore nursery areas
729 originated from areas in the eastern GOA, while the nursery areas to which those individuals
730 dispersed were in the central and western GOA. Typical alongshore dispersal distances from
731 natal to nursery areas were on the order of several hundred kilometers, while the potential for
732 retention or clockwise movement was quite small.

733 The east-to-west connection between putative natal and nursery areas reflects the general
734 circulation patterns in the GOA, which are dominated by counter-clockwise circulation of the
735 Alaska Gyre (Alaskan Stream/Alaska Current system) over the shelf break (Reed, 1984) and the
736 buoyancy-driven Alaska Coastal Current on the shelf (Royer, 1998; Stabeno et al., 2004). The
737 GOA has multiple hydrographic fronts which can hinder on-shelf transport (Belkin et al., 2002,
738 2003). This region is generally thought of as having a downwelling shelf because of the onshore
739 Ekman transport that results from storms generated by the Aleutian Low Pressure system
740 (Weingartner et al., 2005). Previous observations have implicated wind generated Ekman
741 transport in the advection of oceanic zooplankton onto the shelf (Cooney, 1986). Here we have
742 shown that there is sufficient on-shelf advection to transport young POP from deep, off-shelf
743 larval extrusion sites to shallow inshore nursery areas, without the inclusion of any directed
744 horizontal swimming behavior, e.g. towards shallower bathymetry, food, or a particular
745 geographic location.

746 However, while the connectivity patterns from the IBM are consistent with general
747 circulation patterns in the GOA, they are inconsistent with recent genetics studies (Withler et al.,
748 2001; Palof et al., 2011; Kamin et al., 2013) that infer the existence of distinct subpopulations at
749 small spatial scales in the GOA and British Columbia, with the implication that dispersion of
750 POP in the larval and pelagic juvenile stages must be geographically limited (Withler et al.,

751 2001; Palof et al., 2011; Kamin et al., 2013). In the GOA, Palof et al. (2011) found that adult
752 neighborhoods were smaller than their scale of sampling (~400 km), possibly as small as 70 km.
753 Kamin et al. (2013) found similar scales for young-of-the-year POP. The mechanisms
754 contributing to such isolation were unclear, however.

755 Our results indicate that dispersal distances at settlement for passively drifting larvae and
756 pelagic juveniles are on the order of 600 km, and that the potential for retention in areas on the
757 order of 150 km is small, at best. Palof et al. (2011) and Kamin et al. (2013) raised the possibility
758 that oceanographic mechanisms such as entrainment of larvae or pelagic juveniles in gyres and
759 eddies could decrease the extent of transport from natal locations. Our results indicate that
760 entrainment in such features does occur (Fig. 5), even for passively-drifting life stages, and that
761 this may indeed diminish downstream (counter-clockwise) transport of the entrained individuals,
762 particularly from natal sites in the eastern and central GOA. However, other mechanisms must be
763 responsible for limiting the dispersal scales inferred from the genetics sampling.

764 Kamin et al. (2013) also suggested the possibility that active homing may play a role in
765 limiting dispersal distances, and directed swimming by pelagic juvenile rockfish has been
766 suggested. In light of our results that assume essentially passive horizontal drift behavior, it
767 seems highly likely that active behavior at some early life stage must occur to achieve limited
768 dispersal. Adults of some species exhibit homing abilities, returning to reefs from which they
769 were displaced (Carlson and Haight, 1972; Mitamura et al., 2002). Pelagic juveniles of other
770 rockfish species appear to be capable of sustained directed swimming speeds, ignored in our
771 simulations, on the order of 10 cm s^{-1} (Kashef et al., 2014). These would be adequate to counter
772 transport away from natal areas, except in the heart of the Alaskan Coastal Current or the Alaska
773 Stream, where current speeds can reach over 100 cm s^{-1}. It is unknown, though, what cues would

774 provide the necessary directionality for directed swimming to inshore nurseries in the
775 neighborhood of a natal site. A modified version of the IBM could, potentially, provide a
776 relatively inexpensive way of testing the effects of simple (possibly life stage-specific)
777 behavioral rules such as “always swim upstream” or “always swim up the bathymetric gradient”
778 on connectivity and retention.
779
780 *4.3. Environmental indices potentially associated with connectivity*
781
782 Variability in the aggregate connectivity indices we developed appear to be poorly
783 predicted by large-scale environmental indices such as the AO, MEI and PDO. Somewhat
784 surprisingly, the regional-scale indices for cross-shelf flow developed directly from the ROMS
785 models used to drive the IBM were also poor predictors of the aggregate connectivity indices.
786 Considering the dynamic nature of current patterns in the GOA and the resultant complexity of
787 the some of the pathways individuals took in the IBM, it is not surprising that indices based on
788 spatiotemporal quantities defined from an Eulerian perspective (the large-scale environmental
789 and ROMS indices) would not capture what are inherently Lagrangian processes involving fairly
790 large spatial (100’s of km) and temporal (months) scales.
791
792 *4.4. Predicting recruitment*
793
794 Identifying indices that explain 50% or more of the variability in recruitment may
795 improve recruitment estimates from stock assessment models (De Olivera and Butterworth,
796 2005). Here, we tested combinations of the time series of the fraction of individuals, by natal

797 zone, successfully settling in any nursery area across the GOA as potential linear predictors for
798 POP recruitment variability, as estimated in the most recent stock assessment (Hulson et al.,
799 2015). Of the ~300 possible models we evaluated, one had an adjusted $R^2 \geq 50\%$ and was
800 statistically significant (marginally, with $p < 0.05$ after controlling for multiple comparisons;
801 Table 4). However, the regression coefficient for PWS (zone 6), one of the two natal zones
802 included in the model, was negative such that subsequent age-2 recruitment was predicted to be
803 smaller under conditions when more individuals originating from PWS successfully settled in a
804 nursery area somewhere. The veracity of this model, even though marginally significant, is
805 questionable because it seems to imply the action of negative density dependence after
806 settlement in the western GOA (because the IBM predicts successfully-settling larvae extruded
807 in PWS settle to the west). This seems unlikely because nursery habitat appears to be relatively
808 abundant in the western GOA.
809 Thus, variability in recruitment of age 2 POP in the GOA appears to be driven by more
810 than just variability in "maximum potential" connectivity. This suggests that environmentally-
811 mediated changes in mortality and growth along the trajectories of "successful" individuals
812 substantially alter the patterns of "effective" connectivity, obtained by including these biological
813 processes, from those of "maximum potential" connectivity obtained by considering only
814 physical (transport) processes.
815
816 *4.4. Further considerations*
817
818 In this study, we hypothesized that variability in connectivity (i.e. transport) between
819 offshore spawning and inshore nursery areas was the main factor driving juvenile recruitment

820 variability as estimated by the stock assessment model (Hulson et al., 2015). Our results suggest
821 marginal predictive power, at best, for age-2 recruitment to the population using the suite of
822 IBM-related indices we tested. However, this failure to adequately predict recruitment does not
823 negate the value of the IBM, nor of this study.

824 One cannot (yet) reject the hypothesis regarding the relative importance of connectivity
825 on recruitment. There are a number of obvious factors which could contribute to the
826 "disconnect" between the IBM connectivity-based results and recruitment. One factor is that the
827 current model clearly does not incorporate the behavioral mechanisms necessary to achieve the
828 small scales of dispersal inferred from the genetic studies (Palof et al., 2011; Kamin et al., 2013).
829 Another factor is that parturition may vary on an interannual basis in a manner that is not
830 captured in the IBM. The indices we developed from the IBM weight the fraction of successful
831 individuals from a natal zone equally by year, so that substantial interannual variability in the
832 actual number of larvae extruded from a natal zone would degrade any relationship between the
833 indices and recruitment.

834 Additionally, the biological processes captured in the IBM include extremely simple
835 characterizations of larval growth (constant growth rates) and survival (constant). Environmental
836 influences on growth or survival may be important drivers of recruitment variability, as
837 suggested by Stachura et al. (2014). Environmentally-sensitive growth rates could reduce or
838 prolong life stage durations, altering the timing when pelagic stages become competent to settle
839 to the benthos and thus altering connectivity.

840 The last possibility, of course, is that our simplifying hypothesis is wrong and that
841 variability in connectivity is not the major factor in determining recruitment variability as
842 estimated in the stock assessment model. Whether true or not, one could use the IBM to explore

843 the relative importance of transport relative to potential environmental influences on growth or
844 survival along individual pathways, based on hypothesized mechanisms.
845
846
847 **5. Conclusions**
848
849 Our major findings in this study were that, assuming no directed movement by POP prior
850 to the young-of-the-year life stage, : 1) under the influence of multiple eddies and gyres, larval
851 POP in the GOA undergo complex trajectories after extrusion in natal areas along the shelf
852 break, 2) young POP successfully settling in nursery areas throughout the GOA likely originate
853 in the eastern to central GOA, and 3) POP from natal areas in the western GOA likely contribute
854 little to the population in the GOA. The latter two results conflict with genetic studies that
855 suggest dispersal distances are extremely limited and that natal areas in the western GOA
856 contribute to the population in the central GOA (Palof et al., 2011; Kamin et al., 2013). Although
857 our results disagree with these genetic studies, they suggest testable hypotheses for future field
858 work focused on dispersion of pre-settlement POP larvae and pelagic juveniles, as well as the
859 critical requirement for studies on the capabilities of directed swimming by POP during these life
860 stages.
861 We also suggest that, at least in a highly-dynamic system like the GOA, information
862 derived such as on connectivity by following individuals (i.e. from a Lagrangian perspective)
863 will not be simply related to information derived from spatial/temporal averages (i.e. from an
864 Eulerian perspective) because the relevant scales are too diverse.

865 Finally, we are hesitant to recommend the current IBM as a means to provide a suitable

predictive index of recruitment to improve the POP stock assessment model without first addressing several apparent deficiencies, including incorporating directed movement and environmentally-mediated growth rates.

Acknowledgements

This work was funded by the North Pacific Research Board (NPRB)-sponsored GOA Integrated Ecosystem Research Program (GOAIERP) under award #G84. This work was also supported in part by a grant of High Performance Computing resources from the Arctic Region Supercomputing Center. This manuscript is NPRB publication number 671, GOAIERP publication number 29, contribution EcoFOCI-0866 to NOAA's Fisheries-Oceanography Coordinated Investigations, Pacific Marine Environmental Laboratory contribution number 4442, and Alaska Fisheries Science Center publication number 2897. This publication is partially funded by the Joint Institute for the Study of the Atmosphere and Ocean (JISAO) under NOAA Cooperative Agreement NA15OAR4320063, Contribution No.2018-0144. The authors would like to thank K. Hedstrom for her effort in the initial development of the ROMS GOA model on which our experiments were based, as well as A. Punt for his contributions as NPRB's Modeling Coordinator. We would also like to thank K. Shotwell and two anonymous reviewers for their comments and suggestions on the original draft of this paper.

The findings and conclusions in the paper are those of the author(s) and do not necessarily represent the views of the National Marine Fisheries Service. Reference to trade names does not imply endorsement by the National Marine Fisheries Service, NOAA.

888 **References**

889 Ahlstrom, E.H., 1959. Vertical distribution of pelagic fish eggs and larvae off California and
890 Baja California. U.S. Fish and Wildlife Service, Fish. Bull. 60, 107-146.
891 Ainley, D.G., Sydeman, W.J., Parrish, R.H., Lenarz, W.H., 1993. Oceanic factors influencing
892 distribution of young rockfish (*Sebastes*) in central California: A predator's perspective.
893 CalCOFI Report 34, 133-139.
894 Allen, M.J., Smith, G.B., 1988. Atlas and zoogeography of common fishes in the Bering Sea and
895 northeastern Pacific. U.S. Dep. Commer., NOAA Tech. Rept. NMFS 66, 151 p.
896 Belkin, I.M., Krishfield, R., Honjo, S., 2002. Decadal variability of the North Pacific Polar
897 Front: Subsurface warming versus surface cooling. Geophys. Res. Lett. 29(9), 65-1-65-4.
898 Belkin, I.M., Cornillon, P., Ullman, D., 2003. Ocean fronts around Alaska from satellite SST
899 data. In: Proceedings of the American Meteorological Society 7th Conference on Polar
900 Meteorology and Oceanography. Hyannis, MA. Paper 12.7. 15pp.
901 Boehlert, G.W., Gadomski, D.M., Mundy, B.C., 1985. Vertical distribution of ichthyoplankton
902 off the Oregon coast in spring and summer months. Fish. Bull. 83, 611-621.
903 Bond, N.A., Harrison, D.E., 2000. The Pacific Decadal Oscillation, air-sea interaction and
904 central north Pacific winter atmospheric regimes. Geophys. Res. Lett. 27(5), 731-734.
905 Brodeur, R.D., 2001. Habitat-specific distribution of POP (*Sebastes alutus*) in Pribilof Canyon,
906 Bering Sea. Cont. Shelf Res. 21, 207-224.
907 Burnham, K. P.; Anderson, D.R., 2002. Model Selection and Multimodel Inference: A Practical
908 Information-Theoretic Approach, second edition. Springer-Verlag, New York.
909 Calcagno, V., C. de Mazancourt, C., 2010. glmulti: An R Package for Easy Automated Model
910 Selection with (Generalized) Linear Models. J. Stat. Soft. 34.12, 1-29.
911 Carlson, H.R., Haight, R.E., 1972. Evidence for a home site and homing of adult yellowtail
912 rockfish, *Sebastes flavidus*. J. Fish. Res. Board Can. 29, 1011-1014.
913 Carlson, H.R., Haight, R.E., 1976. Juvenile life of POP, *Sebastes alutus*, in coastal fiords of
914 southeastern Alaska: their environment, growth, food habits, and schooling behavior.
915 Trans. Am. Fish. Soc. 105,191-201.
916 Carlson, H.R., Straty, R.R., 1981. Habitat and nursery grounds of Pacific rockfish, *Sebastes* spp.,
917 in rocky coastal areas of Southeastern Alaska. Mar. Fish. Rev. 43, 13-19.
918 Conrath, C.L., Knoth, B., 2013. Reproductive biology of POP in the GOA. Mar. Coast. Fish. 5,
919 21-27.
920 Cooney, R.T., 1986. The seasonal occurrence of *Neocalanus cristatus*, *Neocalanus plumchrus*,
921 and *Eucalanus bungii* over the shelf of the northern GOA. Cont. Shelf Res. 5, 541–553.
922 https://doi.org/10.1016/0278-4343(86)90075-0
923 Cooper, D.W., Duffy-Anderson, J.T., Stockhausen, W.T., Cheng, W., 2013. Modeled
924 connectivity between northern rock sole (*Lepidopsetta polyxystra*) spawning and nursery
925 areas in the eastern Bering Sea. J. Sea Res. 84, 2-12.
926 https://doi.org/10.1016/j.seares.2012.07.001
927 Cowen, R.K., Paris, C.B., Srinivasan, A., 2006. Scaling of Connectivity in Marine Populations.
928 Science 311, 522-527.
929 Cowen, R.K., Gawarkiewicz, G., Pineda, J., Thorrold, S.R., Werner, F.E., 2007. Connectivity in
930 Marine Systems: An Overview. Oceanogr. 20(3), 14-21.
931 Coyle, K., Cheng, W., Hinckley, S.L., Lessard, E.J., Whitledge, T., Hermann, A.J., Hedstrom,
932 K., 2012. Model and field observations of effects of circulation on the timing and

magnitude of nitrate utilization and production on the northern GOA shelf. Prog. Oceanogr. 103, 16-41. https://doi.org/10.1016/j.pocean.2012.03.002.

Coyle, K.O., Gibson, G.A., Hedstrom, K., Hermann, A.J., Hopcroft, R.R., 2013. Zooplankton biomass, advection and production on the northern GOA shelf from simulations and field observations. J. Mar. Sys. 128,185-207, https://doi.org/10.1016/j.jmarsys.2013.04.018

Dai, A., Qian, T., Trenberth, K.E., Milliman, J.D., 2009. Changes in continental freshwater discharge from 1948-2004. J. Climate 22, 2773-2791.

De Olivera, J.A.A., Butterworth, D.S., 2005. Limits to the use of environmental indices to reduce risk and/or increase yield in the South African anchovy fishery. Afr. J. Mar. Sci. 27, 191-203.

Danielson, S., Curchitser, E., Hedstrom, K., Weingartner, T,, Stabeno, P., 2011. On ocean and sea ice modes of variability in the Bering Sea. J. Geophys. Res. 116, C12034. https://doi.org/10.1029/2011JC007389

Dobbins, E.L., Hermann, A.J., Stabeno, P., Bond, N.A., Steed, R.C., 2009. Modeled transport of freshwater from a line-source in the coastal GOA. Deep Sea Res. II 132, 162-193. https://doi.org/10.1016/j.dsr2.2009.02.004

Doyle, M.J., Mier, K.L., 2016. Early life history pelagic exposure profiles of selected commercially important fish species in the Gulf of Alaska. Deep Sea Res. II 132, 162-93. https://doi.org/10.1016/j.dsr2.2015.06.019

Fisher, R., Sogard, S.M., Berkeley, S.A., 2007. Trade-offs between size and energy reserves reflect alternative strategies for optimizing larval survival potential in rockfish. Mar. Ecol. Prog. Ser. 344, 257-270.

Gharrett, A. J., Li, Z., Kondzela, C.M. Kendall, A.W. 2002. Final report: species of rockfish (*Sebastes* spp.) collected during ABL-OCC cruises in the GOA in 1998-2002. (Unpubl. manuscr. available from the NMFS Auke Bay Laboratory, 11305 Glacier Hwy., Juneau AK 99801.)

Gibson, G.A., Stockhausen, W. Coyle, K.O., Hinckley, S., Parada, C., Hermann, A., Doyle, M., Ladd, C, this volume. An individual-based model for Sablefish: Exploring the connectivity between potential spawning and nursery grounds in the Gulf of Alaska. Deep Sea Res. II.

Haidvogel, D.B., and co-authors, 2008. Regional Ocean Forecasting in Terrain-following Coordinates: Model Formulation and Skill Assessment. J. Comput. Phys. 227, 3595-3624.

Haldorson, L, Love, M., 1991. Maturity and fecundity in the rockfishes, *Sebastes* spp., a review. Mar. Fish. Rev. 53(2), 25–31.

Hanselman, D.H., Quinn, T.J., Lunsford, C., Heifetz, J., Clausen, D.M., 2001. Spatial implications of adaptive cluster sampling on GOA rockfish. In: Proceedings of the 17th Lowell- Wakefield Symposium: Spatial Processes and Management of Marine Populations. Univ. Alaska Sea Grant Program, Fairbanks, AK, pp. 303-325.

Hermann, A.J., Curchitser, E.N., Haidvogel , D.B., Dobbins, E.L., 2009a. A comparison of remote versus local influence of El Nino on the coastal circulation of the Northeast Pacific. Deep Sea Res. II 56, 2427-2443. https://doi.org/10.1016/j.dsr2.2009.02.005

Hermann, A.J., Hinckley, S., Dobbins, E.L., Haidvogel, D.B., Bond, N.A., Mordy, C., Kachel, N., Stabeno, P.J., 2009b. Quantifying cross-shelf and vertical nutrient flux in the GOA with a spatially nested, coupled biophysical model. Deep Sea Res. II 56, 2474-2486. https://doi.org/10.1016/j.dsr2.2009.02.008

Hermann, A.J., Ladd, C., Cheng, W., Curchitser, E., Hedstrom, K., 2016. A model-based examination of multivariate physical modes in the GOA. Deep Sea Res. II 132, 68-89. https://doi.org/10.1016/j.dsr2.2016.04.005

Higgins, R.W., Leetmaa, A., Xue, Y., Barnston, A., 2000. Dominant factors influencing the seasonal predictability of U.S. precipitation and surface air temperature. J. Climate 13, 3994-4017.

Higgins, R.W., Leetmaa, A., Kousky, V.E., 2002. Relationships between climate variability and winter temperature extremes in the United States. J. Clim. 15, 1555-1572.

Higgins, R.W., Zhou, Y.,Kim, H.-K., 2001. Relationships between El Niño-Southern Oscillation and the Arctic Oscillation: A Climate-Weather Link. NCEP/Climate Prediction Center ATLAS 8. http://www.cpc.ncep.noaa.gov/research_papers/ncep_cpc_atlas/8/index.html

Hinckley, S., A.J. Hermann and B.A. Megrey, B.A., 1996. Development of a spatially-explicit, individual-based model of marine fish early life history. Mar. Ecol. Prog. Ser. 139:47-68.

Hinckley, S., Hermann, A.J., Mier, K.L., Megrey, B.A., 2001. Importance of spawning location and timing to successful transport to nursery areas: a simulation study of GOA walleye pollock. ICES J. of Mar. Sci. 58, 1042–1052.

Hinckley, S., Coyle, K.O., Gibson, G., Hermann, A.J., Dobbins, E.L., 2009. A biophysical NPZ model with iron for the GOA: Reproducing the differences between an oceanic HNLC ecosystem and a classical northern temperate shelf ecosystem. Deep Sea Res. II 56, 2520-2536. https://doi.org/10.1016/j.dsr2.2009.03.003

Hinckley, S., Stockhausen, W., Coyle, K.O., Laurel, B., Gibson, G.A., Parada, C., Hermann, A., Doyle, M., Hurst, T., this volume. Connectivity between spawning and nursery areas for Pacific cod (*Gadus macrocephalus*) in the Gulf of Alaska. Deep Sea Res. II.

Hulson, P.J.F., Hanselman, D.H., Shotwell, S.K., Lunsford, C.R., Ianelli, J.N., 2015. 9. Assessment of the POP stock in the GOA. In: Appendix B: Stock Assessment and Fishery Evaluation Report for the Groundfish Resources of the GOA. North Pacific Fishery Management Council, 605 W 4th Avenue, Suite 306, Anchorage, AK 99501.

Janout, M.A., Weingartner, T.J., Okkonen, S.R., Whitledge, T.E., Musgrav, D.L., 2009. Some characteristics of Yakutat Eddies propagating along the continental slope of the northern GOA. Deep Sea Res. II 56, 2444–2459. https://doi.org/10.1016/j.dsr2.2009.02.006

Kamin, L.M., Palof, K.J., Heifetz, J., Gharrett, A.J., 2013. Interannual and spatial variation in the population genetic composition of young-of-the-year POP (*Sebastes alutus*) in the GOA. Fish. Oceanogr. 23,1-17.

Kashef, N.S., Sogard, S.M., Fisher, R., Largier, J.L., 2014. Ontogeny of critical swimming speeds for larval and pelagic juvenile rockfishes (*Sebastes* spp., family Scorpoaenidae). Mar. Ecol. Prog. Ser. 500, 231-241.

Kendall, A.W., Lenarz, W.H., 1987. Status of early life history studies of northeast Pacific rockfishes. In: Proceedings of the International Rockfish Symposium. Alaska Sea Grant Report No. 87-2. Anchorage Alaska. p. 99-117.

Kendall, A.W., Kondzela, C., Li, Z., Clausen, D., Gharrett, A.J., 2007. Genetic and morphological identification of pelagic juvenile rockfish collected from the GOA. U.S. Department of Commerce, NOAA Professional Paper NMFS 9, 26 pp.

Kim, J.J., Stockhausen, W., Kim, S., Cho, Y.-K., Seo, G.-H., Lee, J.-S., 2015. Understanding interannual variability in the distribution of, and transport processes affecting, the early life stages of *Todarodes pacificus* using behavioral-hydrodynamic modeling approaches. Prog. Ocean. 138, 571-583. https://doi.org/10.1016/j.pocean.2015.04.003

Ladd, C., Stabeno, P., Cokelet, E.D., 2005. A note on cross-shelf exchange in the northern GOA. Deep Sea Res. II 52, 667–679. https://doi.org/10.1016/j.dsr2.2004.12.022

Ladd, C., Stabeno, P.J., 2009. Freshwater transport from the Pacific to the Bering Sea through Amukta Pass. Geophys. Res. Lett. 36, L14608. https://doi.org/10.1029/2009GL039095

Laidig, T.E., Ralston, S., Bence, J.R., 1991. Dynamics of growth in the early life history of shortbelly rockfish *Sebastes jordani*. Fish. Bull. 89, 611-621.

Larson, R.J., Lenarz, W.H., Ralston, S., 1994. The distribution of pelagic juvenile rockfish of the genus *Sebastes* in the upwelling region off Central California. CalCOFI Rep. 35, 175-221.

Large, W.G., Yeager, S.G., 2008. The global climatology of an interannually varying air-sea flux data set. Clim. Dyn. 33, 341-364.

Large, W.G., McWilliams, J.C., Doney, S.C., 1994. Oceanic vertical mixing: a review and a model with a nonlocal boundary layer parameterization. Rev. Geophys. 32, 363-403.

Lenarz, W.H., Larson, R.J., S. Ralston, S., 1991. Depth distributions of late larvae and pelagic juveniles of some fishes of the California Current. CalCOFI Rep. 32, 41-46.

Lisovenko, L.A. 1964. Distribution of the larvae of the rockfish (*Sebastodes alutus* Gilbert) in the GOA. In: Soviet fisheries investigations in the northeast Pacific. Part III. (Transl. from Russian for Clearinghouse Fed. Sci. Tech. Inform. Springfield, Va., TT67-51205) p. 217-225.

Love M.S., Yoklavich, MM., Thorsteinson, L., 2002. The Rockfishes of the Northeast Pacific. University of California Press, Los Angeles.405 pp.

Mantua, N.J., Hare, S.R., Zhang, Y., Wallace, J.M., Francis, R.C., 1997. A Pacific interdecadal climate oscillation with impacts on salmon production. Bull. Am. Met. Soc. 78, 1069-1079.

Marchesiello, P., McWilliams, J.C., Shchepetkin, A.F., 2001. Open boundary conditions for long-term integration of regional oceanic models. Ocean Model. 3, 1-20.

Matarese, A.C., Blood, D.M., Picquelle, S.J., Benson, J.L., 2003. Atlas of abundance and distribution patterns of ichthyoplankton from the Northeast Pacific Ocean and Bering Sea ecosystems based on research conducted by the Alaska Fisheries Science Center (1972-1996). U.S. Dep. Commer., NOAA Professional Paper, NMFS-1. 281 pp.

Matarese, A.C., Kendall, A.W., Blood, D.M., Vinter, B.M., 1989. Laboratory Guide to Early Life Stages of Northeast Pacific Fishes. U.S. Dep. Commer., NOAA Technical Report NMFS 80. 652 pp.

Megrey, B.A., Hinckley, S., 2001. The effect of turbulence on feeding of larval fishes: a sensitivity analysis using an individual-based model. ICES J. Mar. Sci. 58, 1015-1029.

Mitamura, H., and co-authors, 2002. Evidence of homing of black rockfish *Sebastes inermis* using biotelemetry. Fish. Sci. 68, 1189-1196.

Moser, H.G., Ahlstrom, E.H., Sandknop, E.M., 1977. Guide to the identification of Scorpionfish larvae (family Scorpaenidae) in the Eastern Pacific with comparative notes on species of *Sebastes* and *Helicolenus* from other oceans. U.S. Dep. Commer., NOAA Tech. Rep. NMFS Circ. 402.

NGDC, 1988. Data Announcement 88-MGG-02, Digital relief of the Surface of the Earth. U.S. Dep. Commer., NOAA, National Geophysical Data Center, Boulder, Colorado.

North, E.W., Gallego, A., Petitgas, P., 2009. Manual of recommended practices for modelling physical-biological interactions during fish early life. ICES Coop. Res. Rep. No. 295.

Okkonen, S.R., 2003. Satellite and hydrographic observations of eddy-induced shelf-slope

exchange in the northwestern GOA. J. Geophys. Res. 108, 3033. https://doi.org/10.1029/2002JC001342
Palof, K.J., Heifetz, J., Gharrett, A.J., 2011. Geographic structure in Alaskan POP (*Sebastes alutus*) indicates limited life-time dispersal. Mar. Biol. 158, 779–792.
Parada, C., Armstrong, D.A., Ernst, B., Hinckley, S., Orensanz, J.M., 2010. Spatial dynamics of snow crab (*Chionoecetes opilio*) in the eastern Bering Sea—putting together the pieces of the puzzle. Bull. Mar. Sci. 86, 413-437.
Paris, C.B., K.C. Lindeman, R. Claro, J.L. Fortuna, and R.K. Cowen K. 2004. Modeling Larval Transport from Snapper (*Lutjanidae*) Spawning Aggregations in Cuba. Proc. Gulf Caribb. Fish. Inst. 55, 570-576.
Pelc, R.A.; Warner, R.R., Gaines, S.D., Paris, C.B., 2010. Detecting larval export from marine reserves. Proc. Nat. Acad. of Sci. 107.43 (Oct 26, 2010), 18266-18271.
Preisendorfer, R.W., 1988. Principal Component Analysis in Meteorology and Oceanography. Elsevier Press. 425 pp.
R Core Team, 2015. R: A language and environment for statistical computing. R Foundation for Statistical Computing, Vienna, Austria. http://www.R-project.org/
Reed, R.K., 1984. Flow of the Alaskan Stream and its variations. Deep Sea Res. 31, 369–386.
Royer, T.C., 1982. Coastal freshwater discharge in the northeast Pacific. J. Geophys. Res. 87(C3), 2017-2021.
Royer, T. 1998. Coastal Processes in the Northern North Pacific. In: Brink, K.H., Robinson, A.R. (Ed.s), The Sea, Vol. 11. John Wiley & Sons, New York, p. 395-414.
Saha, S. and coauthors, 2010. The NCEP Climate Forecast System Reanalysis. Bull. Amer. Meteor. Soc. 91, 1015-1057. https://doi.org/10.1175/2010BAMS3001.1
Sakuma, K.M., Laidig, T.E., 1995. Description of larval and pelagic juvenile chilipepper, *Sebastes goodei* (family Scorpaenidae), with an examination of larval growth. Fish. Bull. 93, 721-731.
Sakuma, K.M., Ralston, S., Roberts, D.A., 1999. Diel vertical distribution of postflexion larval *Citharichthys* spp. and *Sebastes* spp. off central California. Fish. Oceanogr. 8, 68-76.
Shchepetkin, A.F., McWilliams, J.C., 2005. The regional oceanic modeling system (ROMS): a split-explicit, free-surface, topography-following-coordinate oceanic model, Ocean Model. 9(4), 347-404.
Stabeno, P.J., N.A. Bond, N.A., Hermann, A.J., Kachel, N.B., Mordy, C.W., Overland, J.E., 2004. Meteorology and oceanography of the northern GOA. Cont. Shelf Res. 24, 859–897.
Stabeno, P.J., Bell, S., Cheng, W., Danielson, S., Kachel, N.B., Mordy, C.W., 2015a. Long-term observations of Alaska Coastal Current in the northern Gulf of Alaska. Deep Sea Res. II 132, 24-40. https://doi.org/10.1016/j.dsr2.2015.12.016
Stabeno, P.J., Bond, N.A., Kachel, N.B., Ladd, C., Mordy, C., Strom, S.L., 2015b. Southeast Alaskan shelf from southern tip of Baranof Island to Kayak Island: Currents, mixing and chlorophyll-a. Deep Sea Res. II 132, 6-23. https://doi.org/10.1016/j.dsr2.2015.06.018
Stabeno, P.J., Reed, R.K., Schumacher, J.D., 1995. The Alaska Coastal Current: Continuity of transport and forcing. J. Geophys. Res. 100(C2), 2477-2485.
Stachura, M.M., Essington, T.E., Mantua, N.J., Hollowed, A.B., Haltuch, M.A., Spencer, P.D., Branch, T.A., Doyle, M.J., 2014. Linking Northeast Pacific recruitment synchrony to environmental variability. Fish. Oceanogr. 23, 389-408.
Stockhausen, W., Hermann, A., 2007. Modeling larval dispersion of rockfish: A tool for marine

reserve design? In: Heifetz, J., DiCosimo, J., Gharrett, A.J., Love, M.S., O'Connell, T., Stanley, R. (Eds.), Biology, assessment, and management of North Pacific rockfishes. Alaska Sea Grant College Program, University of Alaska Fairbanks. p. 251-274.

Stockhausen, W., Lipcius, R., 2001. Single large or several small marine reserves for the Caribbean spiny lobster? Mar. Freshw. Res. 50, 1605-1614.

Stockhausen, W., Lipcius, R., 2003. Simulated effects of seagrass loss and restoration on settlement and recruitment of blue crab postlarvae and juveniles in the York River, Chesapeake Bay. Bull. Mar. Sci. 72, 409-422.

Stockhausen, W., Lipcius, R., Hickey, B., 2000. Joint effects of larval dispersal, population regulation, marine reserve design and exploitation on production and recruitment in the Caribbean spiny lobster. Bull. Mar. Sci.. 66, 957-990.

Stockhausen, W.T., Coyle, K.O., Hermann, A.J., Blood, D., Doyle, M., Gibson, G.A., Hinckley, S., Ladd, C., Parada, C., this volume. Running the gauntlet: connectivity between spawning and nursery areas for arrowtooth flounder (*Atheresthes stomias*) in the Gulf of Alaska, as inferred from a biophysical individual-based model. Deep Sea Res. II.

von Storch, H. and F.W. Zwiers. 1999. Statistical Analysis in Climate Research. Cambridge University Press. 484 pp. http://www.leif.org/EOS/vonSt0521012309.pdf

Weingartner, T.J., Danielson, S.L., Royer, T.C., 2005. Freshwater variability and predictability in the Alaska Coastal Current. Deep Sea Res. II 52, 169-191. https://doi.org/10.1016/j.dsr2.2004.09.030.

Werner F.E., Quinlan, J.A., Lough, R.G., Lynch, D.R., 2001. Spatially-explicit individual based modeling of marine populations: a review of the advances in the 1990s. Sarsia 86, 411-421.

Westrheim, S.J. 1975. Reproduction, maturation, and identification of larvae of some *Sebastes* (Scorpaennidae) species in the northeast Pacific Ocean. J. Fish. Res. Board Can. 32, 2399-2411.

Withler, R.E., Beacham, T.D., Schulze, A.D., Richards, L.J., Miller, K.M.. 2001. Co-existing populations of POP, *Sebastes alutus*, in Queen Charlotte Sound, British Columbia. Mar. Biol. 139, 1-12.

Wolter, K., Timlin, M.S., 1993. Monitoring ENSO in COADS with a seasonally adjusted principal component index. In: Proc. of the 17th Climate Diagnostics Workshop, Norman, OK, NOAA/NMC/CAC, NSSL, Oklahoma Clim. Survey, CIMMS and the School of Meteor., Univ. of Oklahoma. pp. 52-57. http://www.esrl.noaa.gov/psd/enso/mei/WT1.pdf

Wolter, K., Timlin, M.S., 2011. El Niño/Southern Oscillation behaviour since 1871 as diagnosed in an extended multivariate ENSO index (MEI.ext). Intl. J. Climatol. 31, 1074-1087.

Woodbury, D., Ralston, S., 1991. Interannual variation in growth rates and back-calculated birthdate distributions of pelagic juvenile rockfishes (*Sebastes* spp.) of the central California coast. Fish. Bull. 89, 523-533.

Yang, M-S. 1993. Food habits of the commercially important groundfishes in the GOA in 1990. U.S. Dep. Commer., NOAA Tech. Memo. NMFS-AFSC-22 150 p.

Yang, M.-S., Nelson, M.W., 2000. Food habits of the commercially important groundfishes in the GOA in 1990, 1993, and 1996. U.S. Dep. Commer., NOAA Tech. Memo. NMFS-AFSC-112 174 pp.

Yang, M-S., Dodd, K., Hibpshman, R., Whitehouse, A., 2006. Food habits of groundfishes in the GOA in 1999 and 2001. U.S. Dep. Commer., NOAA Tech. Memo. NMFS-AFSC-164

199 pp.
Zhang, Y., Wallace, J.M., Battisti, D.S., 1997. ENSO-like interdecadal variability: 1900-93. J. Climate 10, 1004-1020.

Tables

Table 1. Parameter values used in the Pacific ocean perch IBM.

Table 2. Physical and biological indices derived from ROMS model output. AO: Arctic Oscillation; MEI: Multivariate ENSO Index; PDO: Pacific Decadal Oscillation.

Table 3. Summary of the linear model analysis for the aggregate connectivity indices, as potentially related to the large scale (AO, PDO, and MEI) and ROMS-derived (CSF: cross-shelf flow) environmental indices. All models with 1 or 2 environmental indices as factors were examined; AICc was used to select the "best" model. Only models with adjusted $R2 \geq 0.50$ are shown. ΔAICc is the change in AICc from the best 1-factor model to the best 2-factor model. The p-value, Pr>F, for each model is an empirical family-wise p-value based on the simulating the model fitting process 10,000 times with normally-distributed random time series to obtain the cumulative distribution for the null model.

Table 4. Summary of the linear model analysis for the aggregate connectivity indices as potential predictors for recruitment. We used AICc to select the "best" model, including up to 3 connectivity indices as covariates. ΔAICc is reported for the "best" model (shown) relative to the "best" model with one fewer predictors (negative values indicate a better model). The p-value for the model, Pr>F, is an approximate family-wise p-value based on simulating the model fitting process 10,000 times with normally-distributed random time series to obtain the cumulative distribution for the null model.

Figures

Fig. 1. CGOA ROMS model domain and connectivity zones for the Pacific ocean perch IBM. Alongshore zones are: 1 = PWI (Prince of Wales Island), 2 = Sitka, 3 = Cross Sound, 4 = Yakutat, 5 = Icy Bay, 6 = PWS (Prince William Sound), 7 = Kenai, 8 = North Kodiak, 9 = South Kodiak, 10 = Chirikof, 11 = East Shumagins, 12 = West Shumagins, 13 = Cook Inlet. The inset shows the full CGOA ROMS model domain, with interior grid lines every 50 cells.

Fig. 2. Conceptual model for the Pacific ocean perch IBM. Life stages included in the IBM are: preflexion larva, postflexion larva, pelagic juvenile, settlement-stage juvenile, and benthic juvenile. Larval drawing from Lisovenko (1964). Juvenile drawing from Matarese et al. (1989).

Fig. 3. a) Seasonal patterns of mean abundance of rockfish larvae (*Sebastes* spp.) in tows with non-zero catch in icthyoplankton sampling (bars; Doyle and Mier, 2016). Lines indicate assumed decomposition into Pacific ocean perch (Pacific ocean perch; black) and other (grey) species. b) Seasonality and relative abundance of parturition (release of preflexion individuals) used in the Pacific ocean perch IBM.

Fig. 4. a) Time series from the 2015 GOA Pacific ocean perch stock assessment (Hulson et al., 2015) for recruitment (lagged to parturition year; solid line) and spawning biomass (dotted line). b) Time series of R, $\ln(R)$ and $\ln(R/S)$, standardized as z-scores.

Fig. 5. Trajectories for successful (dark grey) and unsuccessful (light grey) individuals released in 2011 from natal zones 2 (Sitka; upper row), 6 (Prince William Sound; center row), and 10 (Chirikof; bottom row). Left column: trajectories during the preflexion larval stage. Right column: trajectories during later stages.

Fig. 6. a) The fraction of individuals, by natal zone, successfully settling in any nursery zone in the model domain. b) The average alongshore nursery zone, by natal zone, in which successful individuals settled.

Fig. 7. Median (lefthand plot) and root median square deviation (righthand plot) for the annual (1996-2011) connectivity matrices. Nursery areas are plotted west to east (descending order), except for Cook Inlet (alongshore area 13).

Fig. 8. a) The first two EOFs, which account for 60% of the total variance. b) Annual principal component scores for the first two EOFs. Grey boxes indicate $|\text{values}| \leq 0.0001$.

Fig. 9. Time series for the aggregate connectivity indices $C_s(y)$, where s is the natal zone. a) natal zones 1-6; b) natal zones 7-12. Note: y-axis scales are different.

Fig. 10. Comparison of estimated recruitment for POP in the GOA from the 2015 stock assessment (grey circles and line; Hulson et al., 2015) with the "best" model ($R \sim C_2(y) + C_6(y)$; Table 4) predicting recruitment from the aggregate connectivity indices (black diamonds and dashed line). Error bars represent 95% confidence intervals. The adjusted R^2 for the model fit is 0.617.

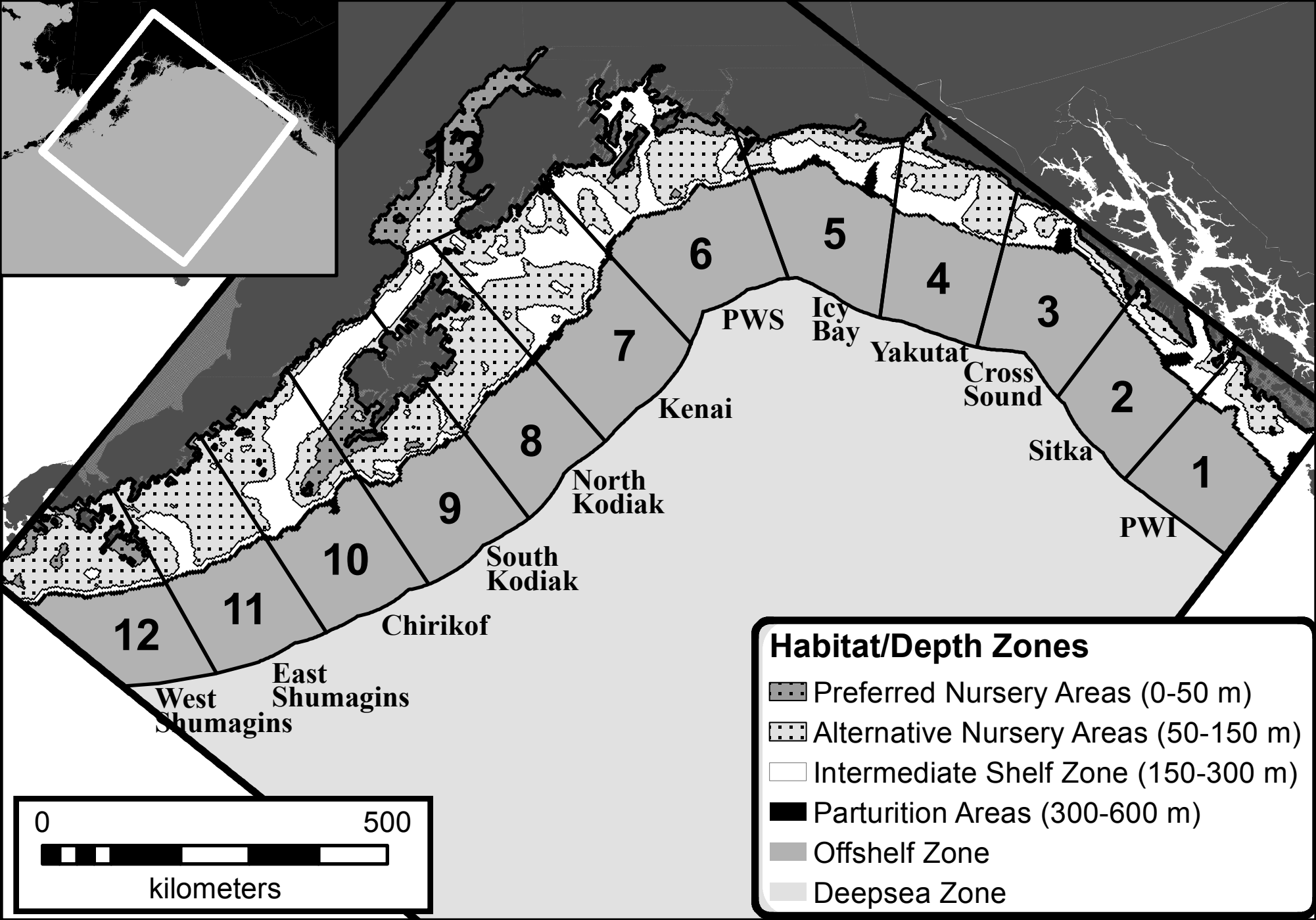
13
6
5
4
3
2
1
7
8
9
10
11
12
PWS
Icy Bay
Yakutat
Cross Sound
Sitka
PWI
Kenai
North Kodiak
South Kodiak
Chirikof
East Shumagins
West Shumagins
0
500
kilometers
Habitat/Depth Zones
Preferred Nursery Areas (0-50 m)
Alternative Nursery Areas (50-150 m)
Intermediate Shelf Zone (150-300 m)
Parturition Areas (300-600 m)
Offshelf Zone
Deepsea Zone

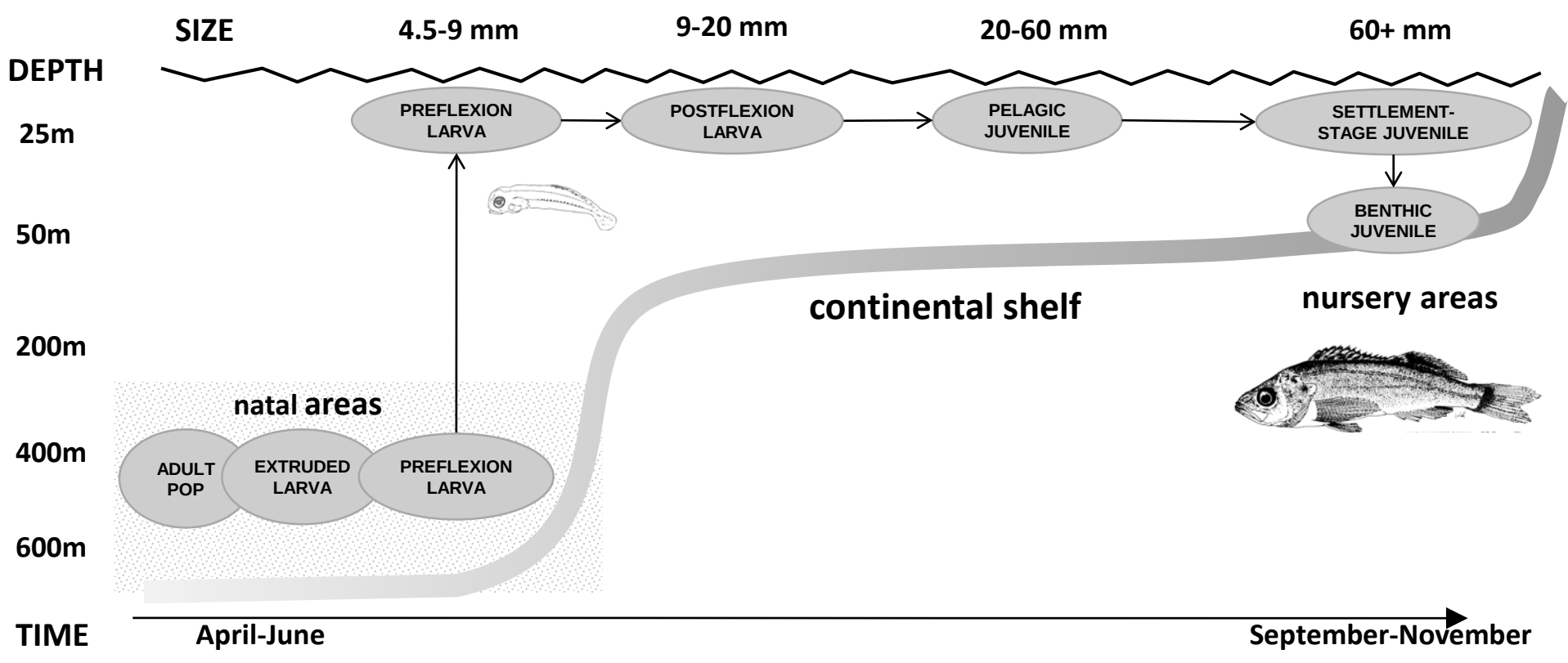
SIZE
4.5-9 mm
9-20 mm
20-60 mm
60+ mm
DEPTH
25m
50m
200m
400m
600m
PREFLEXION LARVA
POSTFLEXION LARVA
PELAGIC JUVENILE
SETTLEMENT-STAGE JUVENILE
BENTHIC JUVENILE
continental shelf
nursery areas
natal areas
ADULT POP
EXTRUDED LARVA
PREFLEXION LARVA
TIME
April-June
September-November

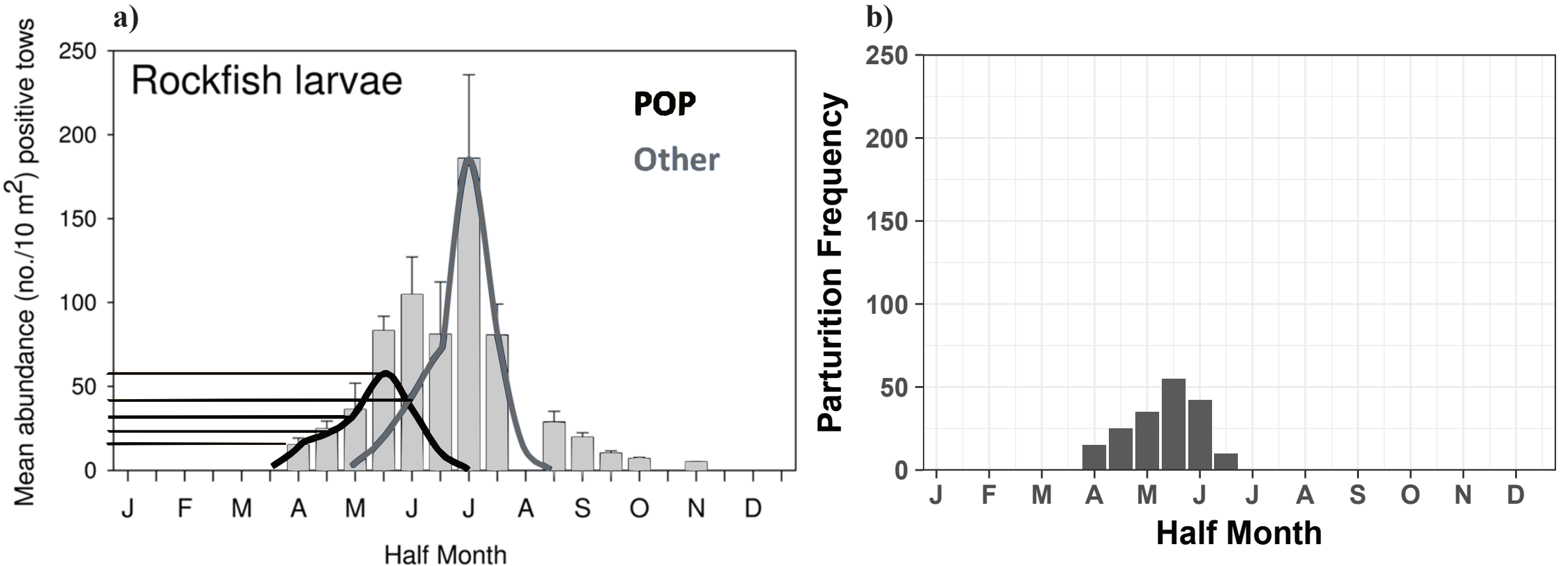
a)
Rockfish larvae
POP
Other
Mean abundance (no./10 m2) positive tows
250
200
150
100
50
0
J F M A M J J A S O N D
Half Month
b)
Parturition Frequency
250
200
150
100
50
0
J F M A M J J A S O N D
Half Month

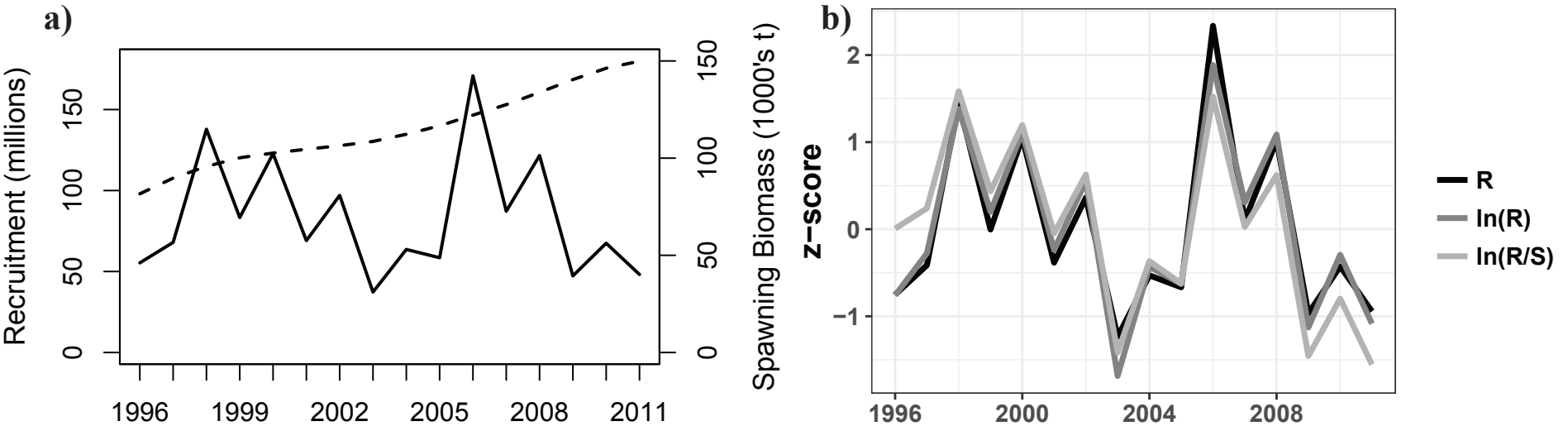
a)
Recruitment (millions)
0
50
100
150
Spawning Biomass (1000's t)
0
50
100
150
1996
1999
2002
2005
2008
2011
b)
z−score
2
1
0
−1
1996
2000
2004
2008
R
ln(R)
ln(R/S)

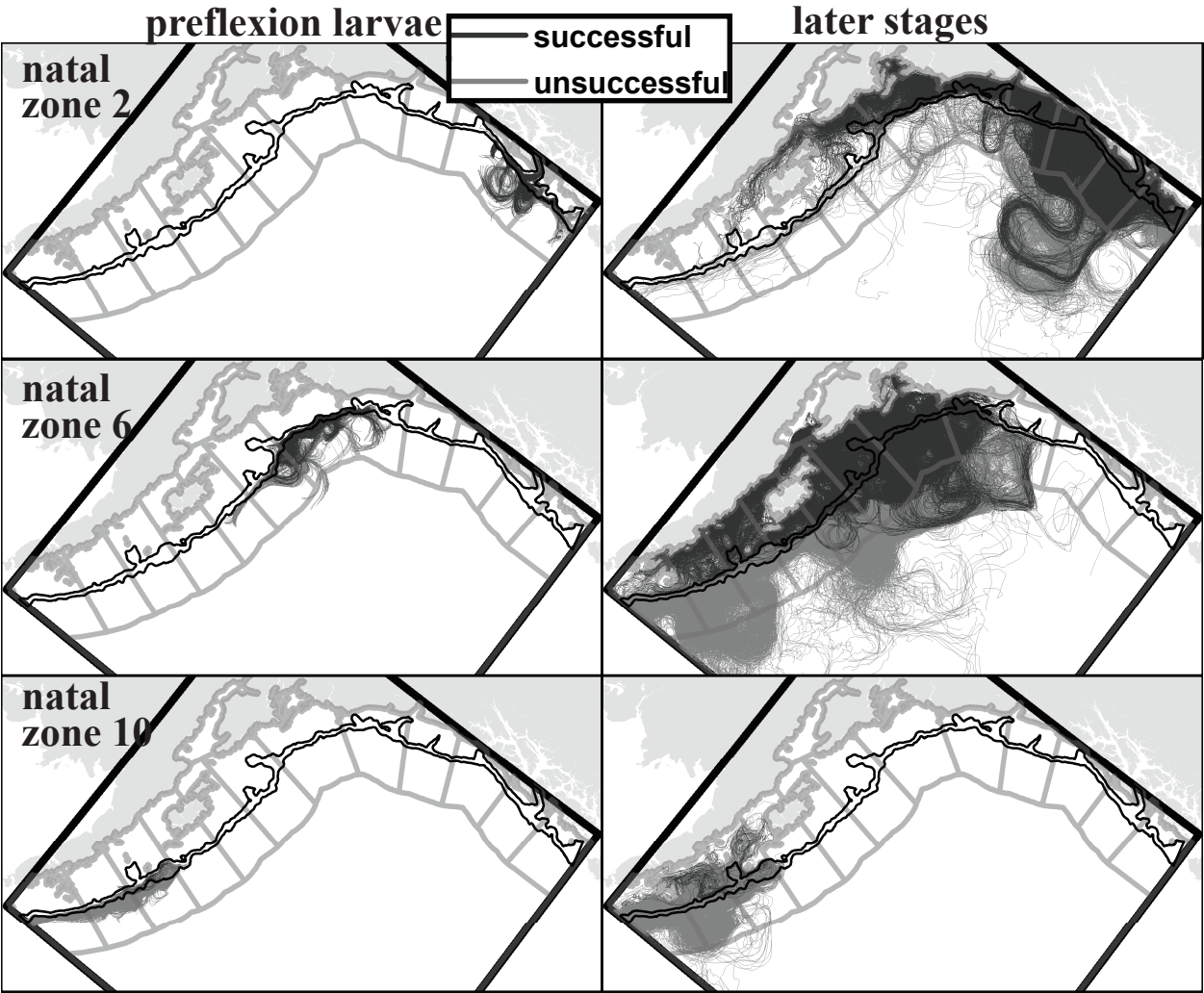
preflexion larvae
later stages
successful
unsuccessful
natal zone 2
natal zone 6
natal zone 10

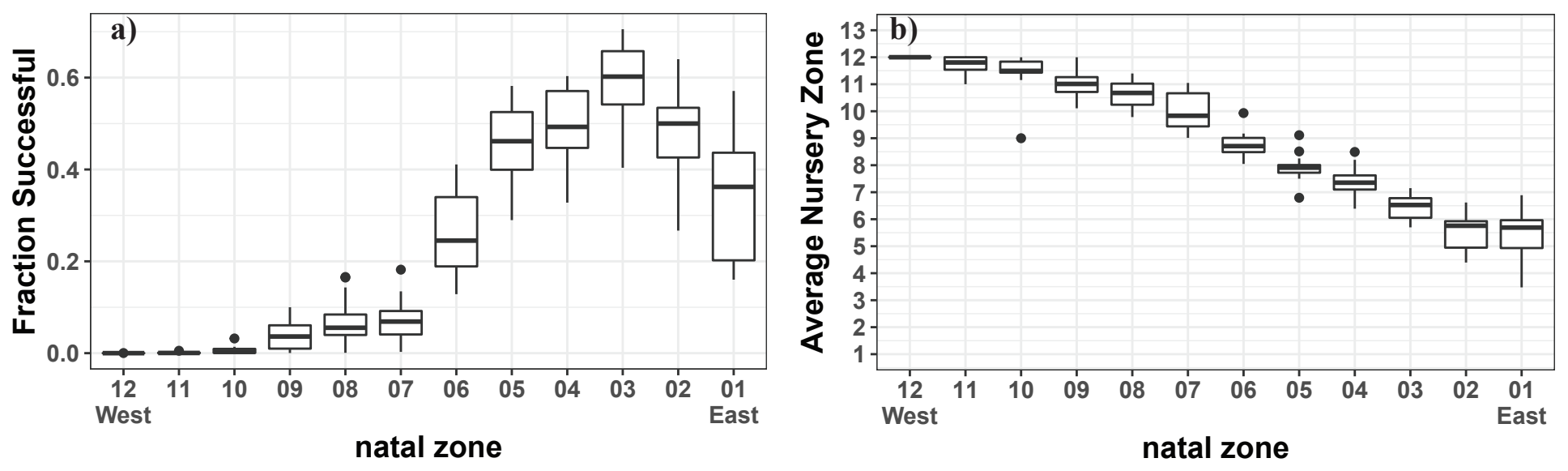
a)
Fraction Successful
0.0
0.2
0.4
0.6
12
11
10
09
08
07
06
05
04
03
02
01
West
East
natal zone
b)
Average Nursery Zone
1
2
3
4
5
6
7
8
9
10
11
12
13
12
11
10
09
08
07
06
05
04
03
02
01
West
East
natal zone

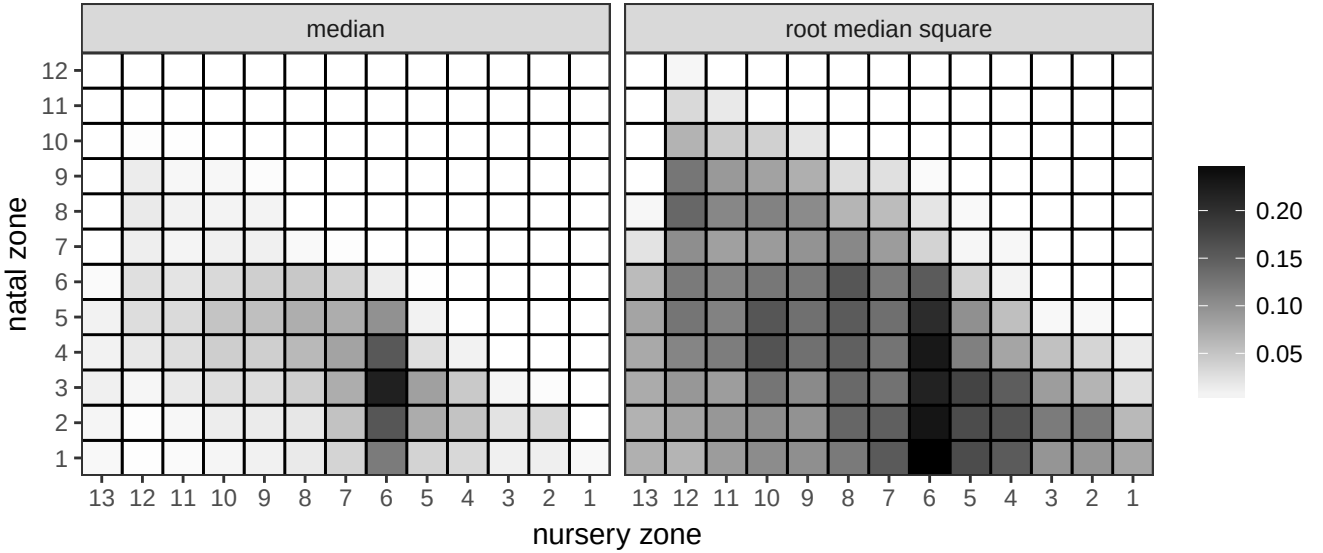
median
root median square
natal zone
nursery zone
12
11
10
9
8
7
6
5
4
3
2
1
13 12 11 10 9 8 7 6 5 4 3 2 1
0.20
0.15
0.10
0.05

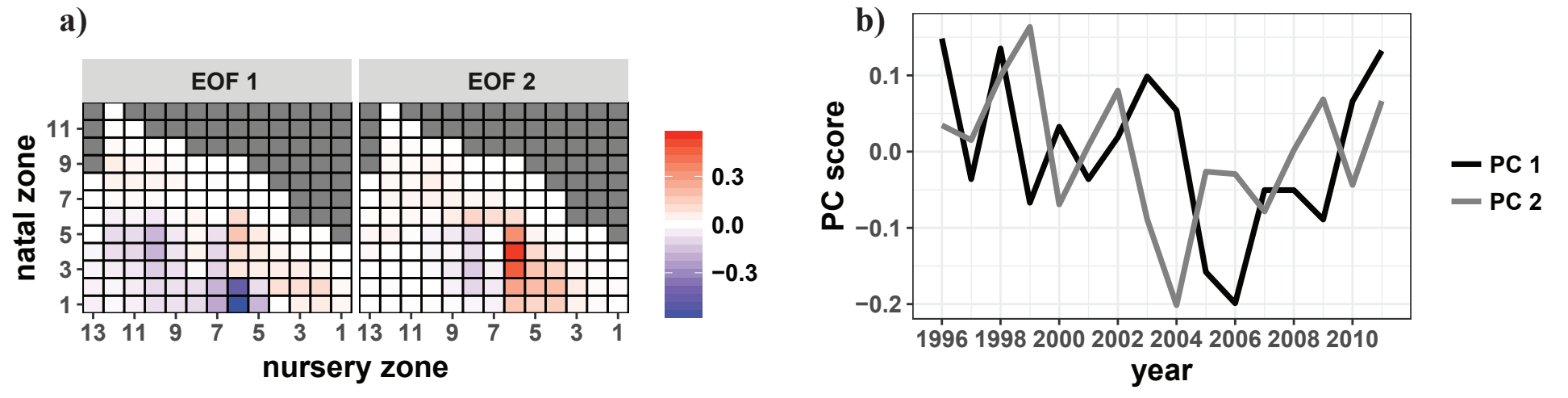
a)
EOF 1
EOF 2
natal zone
11
9
7
5
3
1
13 11 9 7 5 3 1
nursery zone
0.3
0.0
−0.3
b)
PC score
0.1
0.0
−0.1
−0.2
1996 1998 2000 2002 2004 2006 2008 2010
year
PC 1
PC 2

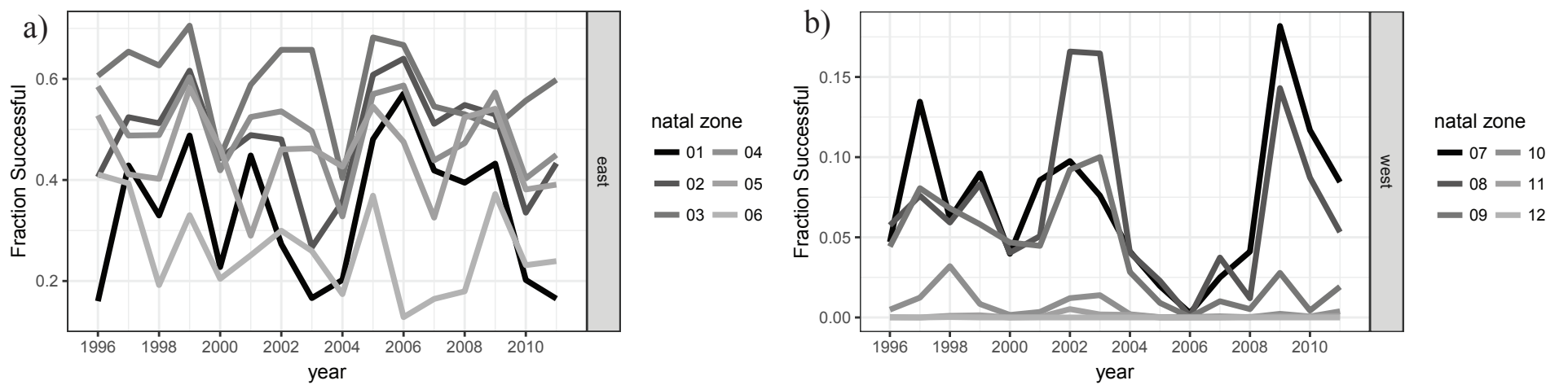
a)
Fraction Successful
0.6
0.4
0.2
1996
1998
2000
2002
2004
2006
2008
2010
year
east
natal zone
01
02
03
04
05
06
b)
Fraction Successful
0.15
0.10
0.05
0.00
1996
1998
2000
2002
2004
2006
2008
2010
year
west
natal zone
07
08
09
10
11
12

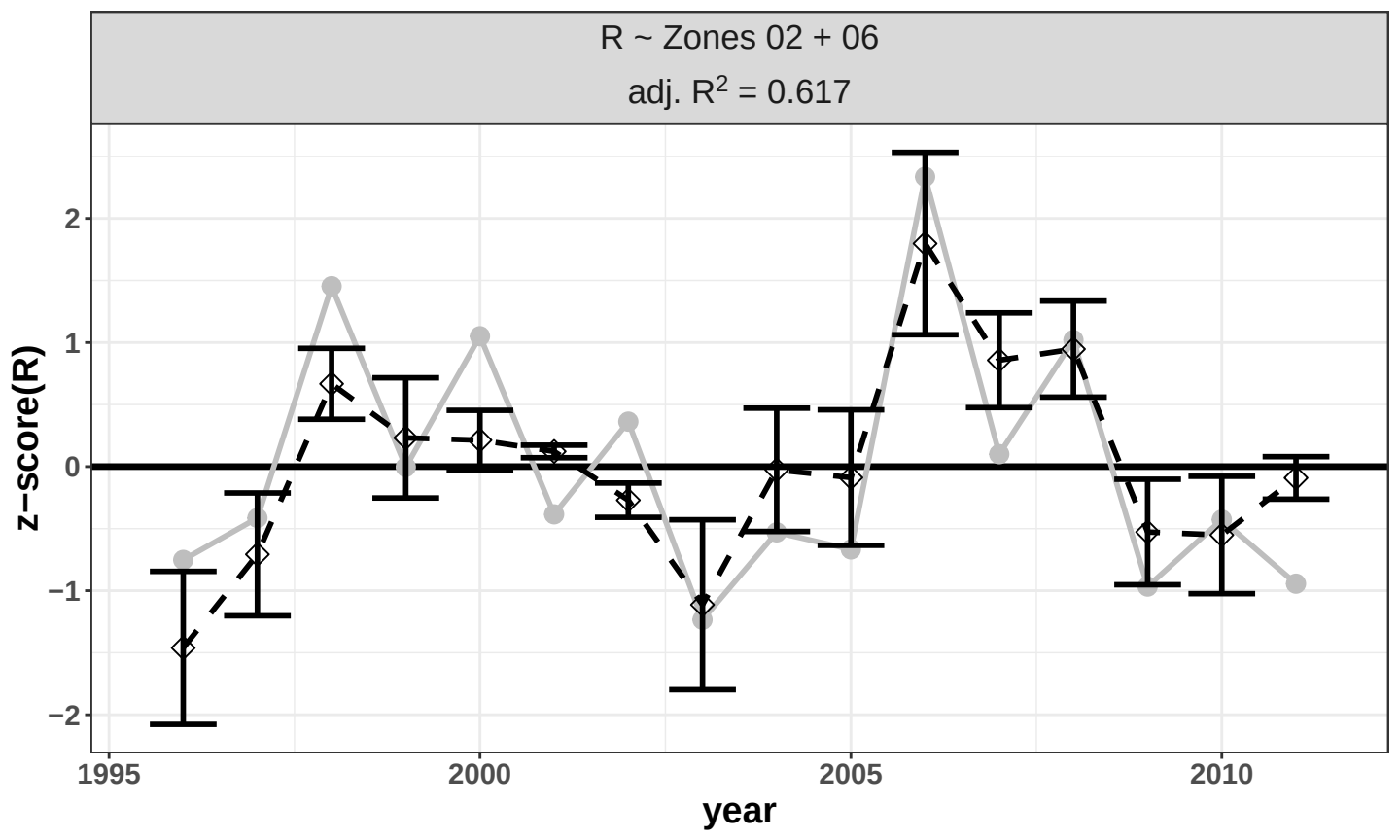
R ~ Zones 02 + 06
adj. R2 = 0.617
z−score(R)
2
1
0
−1
−2
1995
2000
2005
2010
year

Table 1. Parameter values used in the Pacific ocean perch IBM.

Life Stage	Parameter	Value	Units	Description	Based on
Preflexion Larva	z_i	4.5	mm	initial size	[1], [2], [3]
	z_f	9	mm	final size	[3]
	g	0.16	mm/d	growth rate	see text
	d_{min}	300	m	min depth	[4]
	d_{max}	700	m	max depth	[4]
	v_s	1	mm/s	swimming speed	[5], [6]
	D_v	0.0001	m^2/s	vertical diffusivity	
	D_h	0.001	m^2/s	horizontal diffusivity	
	T_{max}	--	days	max. stage duration	(effectively 27.9 days)
Postflexion Larva	z_i	9	mm	initial size	[3], [5]
	z_f	20	mm	final size	[2], [1], [3]
	g	0.34	mm/d	growth rate	see text
	d_{min}	5	m	min depth	[7]
	d_{max}	40	m	max depth	[7], [8], [9]
	v_s	5	mm/s	swimming speed	[5]
	D_v	0.0001	m^2/s	vertical diffusivity	
	D_h	0.001	m^2/s	horizontal diffusivity	
	T_{max}	--	days	max. stage duration	(effectively 32.1 days)
Pelagic Juvenile	z_i	20	mm	initial size	[2], [1], [3]
	z_f	60	mm	final size	[3]
	g	0.44	mm/d	growth rate	based on duration from [2]
	d_{min}	5	m	min depth	[2]
	d_{max}	40	m	max depth	[8], [9]
	v_s	5	mm/s	swimming speed	[5]
	D_v	0.001	m^2/s	vertical diffusivity	
	D_h	0.01	m^2/s	horizontal diffusivity	
	T_{max}	90	days	max. stage duration	[2]
Settlement-stage Juvenile	z_i	60	mm	initial size	[3]
	z_f	60	mm	final size	
	g	0	mm/d	growth rate	
	d_{min}	5	m	min depth	
	d_{max}	50	m	max depth	
	v_s	5	mm/s	swimming speed	[5]
	D_v	0.001	m^2/s	vertical diffusivity	
	D_h	0.01	m^2/s	horizontal diffusivity	
	T_{max}	30	days	max. stage duration	

[1]Kendall and Lenarz, 1987; [2]Matarese et al., 1989; [3]Moser et al., 1977; [4]Love et al., 2002; [5]Kashef et al., 2014; [6]Fisher et al., 2007; [7]Doyle and Mier, submitted; [8]Ahlstrom, 1959; [9]Sakuma et al., 1999.

Table 2. Environmental indices considered as potential factors driving IBM-predicted successful settlement.

type	index	region	season	no. of indices
Large-scale indices	$\begin{Bmatrix}\text{AO}\\ \text{MEI}\\ \text{PDO}\end{Bmatrix}$	--	$\begin{Bmatrix}spring\\ summer\\ fall\end{Bmatrix}$	9
ROMS-derived indices	cross-shelf flow (CSF)	$\begin{Bmatrix}\text{eastern GOA}\\ \text{central GOA}\\ \text{western GOA}\end{Bmatrix}$	$\begin{Bmatrix}spring\\ summer\\ fall\end{Bmatrix}$	9

Table 3. Summary of the linear model analysis for the aggregate connectivity indices, as potentially related to the large scale (AO, PDO, and MEI) and ROMS-derived (CSF: cross-shelf flow) environmental indices. All models with 1 or 2 environmental indices as factors were examined; AICc was used to select the "best" model. Only models with adjusted $R^2 \geq 0.50$ are shown. $\Delta AICc$ is the change in AICc from the best 1-factor model to the best 2-factor model. The p-value, $\Pr(> F)$, for each model is an empirical family-wise p-value based on the simulating the model fitting process 10,000 times with normally-distributed random time series to obtain the cumulative distribution for the null model.

Connectivity Index Type	Zone/PC	Selected Covariate(s)	Coefficient	F value	$\Pr(> F)$	R^2	Adjusted R^2	AICc	$\Delta AICc$
$C_s\ (y)$	Zone 01	CSF eastern GOA-spring AO-spring	0.730 -0.461	14.55	0.06	0.69	0.64	32.1	-4.6
PC	1	CSF eastern GOA-spring AO-spring	-0.616 0.482	8.42	0.31	0.56	0.50	37.3	-3.2

Table 4. Summary of the linear model analysis for the aggregate connectivity indices as potential predictors for recruitment. We used AICc to select the "best" model, including up to 3 connectivity indices as covariates. $\Delta AICc$ is reported for the "best" model (shown) relative to the "best" model with one fewer predictors (negative values indicate a better model). The p-value for the model, $\Pr(> F)$, is an approximate family-wise p-value based on simulating the model fitting process 10,000 times with normally-distributed random time series to obtain the cumulative distribution for the null model.

Connectivity Index Type	Zone	Coefficient	F value	$\Pr(> F)$	R^2	Adjusted R^2	AICc	$\Delta AICc$
$C_s(y)$	02 06	0.5510 -0.6407	13.88	0.044	0.66	0.62	34.9	-7.2